

Electrochemical CO2 Reduction: Commercial Innovations and Prospects

*Original*

Electrochemical CO2 Reduction: Commercial Innovations and Prospects / Varhade, S., Guruji, A., Singh, C., Cicero, G., Garcíamelchor, M., Helsen, J., Pant, D.. - In: CHEMELECTROCHEM. - ISSN 2196-0216. - 12:2(2025).  
[10.1002/celc.202400512]

*Availability:*

This version is available at: 11583/2995972 since: 2024-12-27T16:52:26Z

*Publisher:*

John Wiley and Sons

*Published*

DOI:10.1002/celc.202400512

*Terms of use:*

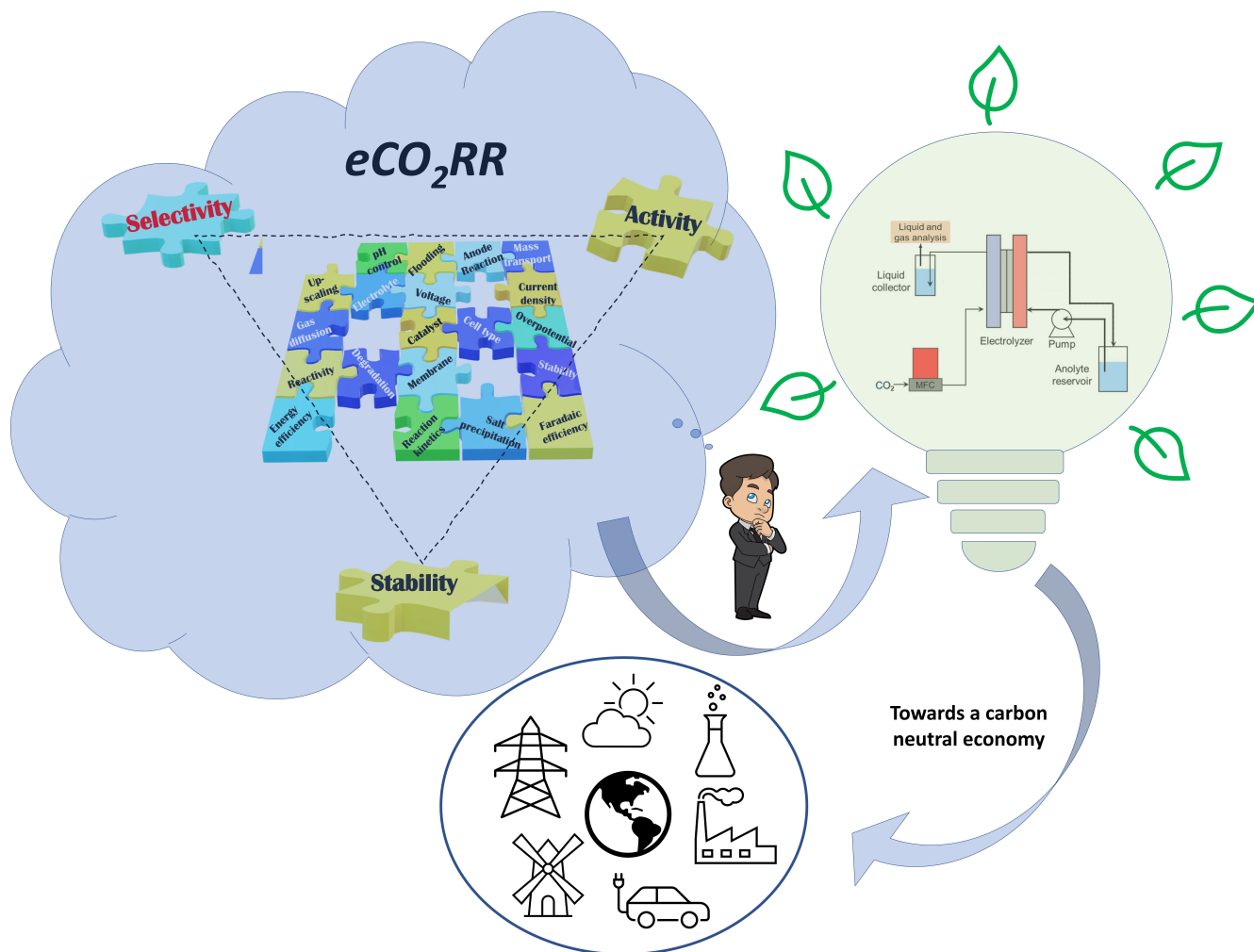
This article is made available under terms and conditions as specified in the corresponding bibliographic description in the repository

*Publisher copyright*

(Article begins on next page)

# Electrochemical CO<sub>2</sub> Reduction: Commercial Innovations and Prospects

Swapnil Varhade<sup>+, [a]</sup>, Avni Guruji<sup>+, [a, b, c]</sup>, Chandani Singh,<sup>[a]</sup> Giancarlo Cicero,<sup>[c]</sup>  
Max García-Melchor,<sup>[b, e, f]</sup> Joost Helsen,<sup>\*, [a]</sup> and Deepak Pant<sup>\*, [a, d]</sup>



Sustainability is an imperative requirement in this era, with electrocatalytic power into fuels technologies emerging as a significant route toward sustainable chemistry. One of the focus areas within the chemical industry is capture of carbon dioxide (CO<sub>2</sub>) and its electrochemical reduction (eCO<sub>2</sub>RR) into economically viable commodities through the utilization of renewable sources. Despite some specific eCO<sub>2</sub>RR technologies being poised for market introduction, the development of a comprehensive technology for eCO<sub>2</sub>RR remains a challenge. While certain technologies targeting specific eCO<sub>2</sub>RR products are on the verge of deployment, substantial efforts are still necessary to transition and establish presence in the market over conventional technologies. This review highlights recent technological

advancements, fundamental studies, and the persisting challenges from an industrial perspective. We take a deep dive into the research methodologies, strategies, challenges, and advancements in the development of applications for eCO<sub>2</sub>RR. Specifically, three eCO<sub>2</sub>RR products – CO, HCOOH, and C<sub>2</sub>H<sub>4</sub> – as promising candidates for implementation are elaborated based on techno-economic considerations. Additionally, the review discusses the industrial blueprint for these products, aiming to streamline their path toward commercialization. The intent is to present the status of eCO<sub>2</sub>RR, offering insights into its potential transformation from a mere laboratory curiosity to a feasible technology for industrial chemical synthesis.

## 1. Introduction

During the Industrial Revolution, the transition in energy sources facilitated substantial technological advancements benefiting humanity. This era marked a pronounced surge in energy demand, predominantly met by fossil fuels, resulting in a significant upsurge in atmospheric CO<sub>2</sub> emissions, notably reaching 424 ppm last year 2023, in stark contrast to the stable pre-industrial revolution levels of around 280 ppm.<sup>[1]</sup> The increased CO<sub>2</sub> concentration has culminated in global temperature rise. To mitigate emissions and meet energy demands, exploration into alternative energy sources has intensified. Specifically, the electrocatalytic CO<sub>2</sub> reduction reaction (eCO<sub>2</sub>RR) has garnered substantial attention.<sup>[2–5]</sup> Diverse methodologies such as photocatalysis, electrocatalysis, biocatalysis, and dry reforming have been proposed to promote CO<sub>2</sub>RR.<sup>[3,5]</sup> Among

these, eCO<sub>2</sub>RR presents a promising avenue due to its ability to operate under mild conditions, regulate reaction rates, and selectively form valuable products, offering potential for sustainable CO<sub>2</sub> utilization. Presently, electrolyzers for eCO<sub>2</sub>RR encompass both high-temperature (>600 °C) solid oxide systems and low-temperature (25–80 °C) variants.<sup>[6–10]</sup> Low-temperature electrolysis exhibits enhanced operational convenience and flexibility, showcasing potential to produce multicarbon compounds like ethylene, ethanol, and propanol.<sup>[5,9,11,12]</sup> Therefore, advances in technology for capturing atmospheric CO<sub>2</sub> and converting it via renewable energy sources into syngas, olefins, alcohols, and acids with low-temperature electrolysis is progressing towards commercial viability.

In conventional laboratory settings, the focus of electrocatalysis revolves around deciphering the interrelation between physical attributes of the electrocatalyst and its electrocatalytic performance. Beyond this, the dynamic behavior of intermediates along with reactants and products within the reaction environment has also been explored.<sup>[13–16]</sup> Conventional electrochemical techniques offer insights into the general characteristics and enduring stability of electrocatalyst materials. However, catalytic activity is influenced by multifaceted factors enveloped within a wide spectrum of parameters, posing challenges in unravelling the fundamental origins of this activity and hindering catalyst advancement.<sup>[14,15]</sup> Unearthing non-obvious information about active sites and elucidating their correlation with electrocatalytic performance (structure-property relationships) is crucial for comprehending the underpinnings of catalytic materials intrinsic to eCO<sub>2</sub>RR. To harness the potential of eCO<sub>2</sub>RR technologies on a larger scale, there is a requisite to upscale the production of chemicals and fuels, necessitating the development of an ecosystem wherein foundational eCO<sub>2</sub>RR studies conducted in laboratories are integrated into scalable technologies.<sup>[2,6]</sup> Expediting progress requires an efficient assessment to address the challenges inherent in eCO<sub>2</sub>RR systems, especially concerning their application in industrial settings. Despite significant advances in our fundamental understanding of catalysis and reaction mechanisms, the transition of present eCO<sub>2</sub>RR systems to industrial scale demands substantial advancements.

Achieving specific performance goals is crucial in the practical application of eCO<sub>2</sub>RR. These benchmarks primarily

[a] S. Varhade,<sup>†</sup> A. Guruji,<sup>†</sup> C. Singh, J. Helsen, D. Pant  
 Electrochemistry Excellence Centre (ELEC), Materials & Chemistry Unit,  
 Flemish Institute for Technological Research (VITO), Boeretang 200, Mol  
 2400, Belgium  
 E-mail: deepak.pant@vito.be  
 joost.helsen@vito.be

[b] A. Guruji,<sup>†</sup> M. García-Melchor  
 School of Chemistry, CRANN and AMBER Research Centres, Trinity College  
 Dublin, College Green, Dublin 2, Dublin, Ireland

[c] A. Guruji,<sup>†</sup> G. Cicero  
 Dipartimento di Scienza Applicata e Tecnologia, Politecnico di Torino,  
 Torino 10129, Italy

[d] D. Pant  
 Centre for Advanced Process Technology for Urban Resource Recovery  
 (CAPTURE), Frieda Sayesstraat 1, Zwijnaare 9052, Belgium

[e] M. García-Melchor  
 Center for Cooperative Research on Alternative Energy (CIC EnergiGUNE),  
 Basque Research and Technology Alliance (BRTA), Alava Technology Park,  
 Albert Einstein 48, 01510 Vitoria-Gasteiz, Spain.

[f] M. García-Melchor  
 IKERBASQUE, Basque Foundation for Science, Plaza de Euskadi 5, 48009  
 Bilbao, Spain.

[†] Equal contribution

Supporting information for this article is available on the WWW under  
<https://doi.org/10.1002/celec.202400512>

© 2024 The Authors. ChemElectroChem published by Wiley-VCH GmbH. This is an open access article under the terms of the Creative Commons Attribution License, which permits use, distribution and reproduction in any medium, provided the original work is properly cited.

involve reaching a current density of over  $200 \text{ mA cm}^{-2}$  while ensuring stability for prolonged periods, ideally exceeding 10,000 hours. Some  $\text{eCO}_2\text{RR}$  products, such as carbon monoxide (CO) and formic acid (HCOOH), have shown impressive stability with selectivities over 90% and current densities surpassing  $200 \text{ mA cm}^{-2}$  for more than 1,000 hours.<sup>[2,12,17]</sup> However, the formation of  $\text{C}_{2+}$  products, which possess greater energy

density and market value, exhibit lower current densities and selectivities compared to  $\text{C}_1$  products. Consequently, there is an urgent need to enhance the current density and selectivity of  $\text{C}_{2+}$  products derived from  $\text{eCO}_2\text{RR}$ , which remains a significant challenge.

When choosing an  $\text{eCO}_2\text{RR}$  system for commercial use, several crucial factors must be considered:



Swapnil Varhade received his Ph.D. (Dr. rer. nat.) in Chemistry under supervision of Professor Wolfgang Schuhmann from Ruhr University Bochum (Germany) in 2022. He was enrolled at International Max Planck Research School for Interface Controlled Materials for Energy Conversion (IMPRS-SURMAT). He is now working as Postdoc Electrochemical Process Engineering at VITO Mol (Belgium). His Ph.D. research work mainly includes electrochemical interface characterization of nanostructured materials using SECCM for electrocatalysis and energy storage/conversion devices. He is currently working on European research projects by contributing to developing, optimizing electrochemical  $\text{CO}_2$  electrolyzer technologies for sustainable fuel production with industrial and academic partners.



Avni Gurujii is a Marie Curie PhD fellow conducting her research studies at the Flemish Institute for Technological Research (VITO) in Belgium, while being enrolled at Politecnico di Torino, Italy. Her research is part of the Marie Skłodowska-Curie European Training Network (MSCA-ETN) ECOMATES project, where she is working on the development and scaling up of gas diffusion electrodes (GDEs) and bimetallic electrocatalysts to advance electrochemical  $\text{CO}_2$  reduction technologies. She pursued a Master's degree from Savitribai Phule Pune University (SPPU), India with a specialization in Inorganic Chemistry (2020-2022). During her master's, she worked on synthesis, characterization, and applications of nickel selenide.



Dr. Chandani Singh received her PhD in chemistry in 2021 from the University of Hyderabad, India. Her PhD research work focused on molecular catalyst development for electrocatalytic water splitting. In 2021-2022, she did her postdoctoral research in collaborative venture between Ariel University and Sami Shamoon College of Engineering, Israel, focusing on electrode development for electrocatalytic water splitting process. She is currently working as a postdoctoral researcher at VITO, Belgium working on projects associated with  $\text{CO}_2$  electrochemical reduction to  $\text{C}_1\text{-C}_2+$  products.



Giancarlo Cicero received a M.S. degree in Chemistry from the University of Torino in 1997 and obtained a Ph.D. in Physics from the Politecnico di Torino in 2003. In 2004, he worked as a postdoctoral fellow at the Lawrence Livermore National Laboratory, where he studied the properties of water in confined media. Since October 2008, he has been working at the Politecnico di Torino, where he is now a full professor in the Structure of Matter. His research activity is devoted to ab initio simulations of surfaces, interfaces, and nanostructured materials with applications in renewable energy system and sustainable processes.



Dr. Max García-Melchor is an Ikerbasque Research Professor at CIC EnergiGUNE, where he leads the Atomistic & Molecular Modelling for Catalysis group. His research leverages advanced computational methods and artificial intelligence to accelerate the discovery of catalytic systems for sustainable chemical and fuel production. With a PhD in Chemistry from the Universitat Autònoma de Barcelona and over 15 years of experience, he specializes in modelling (electro)catalytic reaction mechanisms and developing rational catalyst design approaches.



Joost Helsen is project manager responsible for the upscaling portfolio of projects at the Electrochemistry Excellence Centre at VITO. He has been involved in several European (H2020/Horizon Europe) and national projects on  $\text{CO}_2$  electroreduction, organic electrocatalysis and capacitive deionization. He was responsible for the 5 kW  $\text{CO}_2$  electrolyzer stack built in LOTER.CO2M Project, a 50 kW  $\text{CO}_2$  electrolyzer in ECO2FUEL project and a 1  $\text{m}^2$  pilot for sugar oxidation in the SPIRE project PERFORM.



Dr. Deepak Pant is senior scientist and project manager at projects at the Electrochemistry Excellence Centre at Flemish Institute for Technological Research (VITO), Belgium working on electrosynthesis and resource recovery, specifically, the design and optimization of electrochemical systems for  $\text{CO}_2$  conversion and microbial electrosynthesis. He has a PhD in environmental biotechnology and has 200 peer-reviewed publications, 6 edited books, 9 patents and 40 book chapters to his credit. He is the Editor of Bioresource Technology Reports and Journal of Environmental Chemical Engineering.

1. Operational convenience: The system should be user-friendly and scalable, allowing specific control through electrolysis parameters.
2. Energy efficiency: It should operate with low power density/cell voltage while demonstrating high efficiency in producing various CO<sub>2</sub> reduction products.
3. Product specificity: The system should exhibit high selectivity for the desired product, ideally achieving  $\geq 90\%$  efficiency.
4. Technological readiness: The system should have a high Technology Readiness Level (TRL), indicating its maturity and readiness for commercial deployment.
5. Sustainability: The system should be powered directly from renewable sources like solar, wind, or geothermal, ensuring sustainability.
6. Cost-effectiveness: Consideration should be given to the system's cost, favoring materials suitable for large-scale usage and affordability.

These factors collectively contribute to the viability and suitability of an eCO<sub>2</sub>RR cell configuration for practical, large-scale applications in industry. Considering these parameters, low temperature eCO<sub>2</sub>RR has significant market.

During recent years, considerable work has focused on eCO<sub>2</sub>RR, and several excellent reviews have summarized the eCO<sub>2</sub>RR.<sup>[7,8,18–21]</sup> Most of them, however, have focused on how to design, prepare, and optimize eCO<sub>2</sub>RR catalysts to increase their utilization and conversion rate of CO<sub>2</sub>, improve energy efficiency, and enhance product selectivity. Technical (thermodynamic and kinetic) and practical (infrastructural) hurdles in industrialized eCO<sub>2</sub>RR have also been discussed in the literature.<sup>[22–25]</sup> Some targeted strategies have been put forward to bridge the gap between lab and industry, with some recent reviews focusing on the potential and demand for industrial applications of eCO<sub>2</sub>RR. Therefore, we focus here on a combined approach including recent research, strategies, challenges, and pathways toward industrial applications of eCO<sub>2</sub>RR. To avoid repetition and keep the focus on most promising products, we focus on three main eCO<sub>2</sub>RR products, namely CO, HCOOH, and ethylene (C<sub>2</sub>H<sub>4</sub>), which have been identified as promising targets for industrial applications under the current techno-economic conditions. Their most recent industrial scheme is discussed to pave the way toward commercialization.

## 2. Fundamentals of eCO<sub>2</sub>RR and Economic Analysis of Reaction Products

### 2.1. CO<sub>2</sub> Properties and Reduction Products

CO<sub>2</sub> is among the most stable molecules (thermodynamically), characterized by a robust C=O double bond, boasting a higher bond dissociation energy compared to C–H and C–C bonds.<sup>[26–28]</sup> Electrochemical processes necessitate overcoming the substantial activation energy required to break the C=O bond, and electrocatalysts play a pivotal role in reducing this

barrier, expediting reactions and/or enhancing selectivity towards the desired eCO<sub>2</sub>RR products.<sup>[29–31]</sup> The reaction occurs at the electrode/electrolyte interface and typically involves four main steps: i) CO<sub>2</sub> adsorption on the electrocatalyst surface, ii) C–O bond cleavage or C–H bond formation or O–H bond formation through electron transfer and/or proton-coupled electron transfer steps iii) C–C bond formation, the most challenging step, to form different C<sub>2+</sub> hydrocarbons and oxygenates, and iv) rearrangement of product configuration to desorb from the electrocatalyst surface and diffuse into the electrolyte.<sup>[32,33]</sup> Effective electrocatalysts form chemical bonds with intermediates, decreasing the activation energy for the reaction to occur. The reduction of CO<sub>2</sub> to products that come from a single reaction intermediate can be efficiently achieved, depending upon the specific product.<sup>[34]</sup> However, an increase in the number of electrons involved in the reaction introduces a complex series of steps. Different pathways, intermediates formed, as well as the number of protons and electrons transferred, contribute to a spectrum of products. These encompass C<sub>1</sub> products, like CO, HCOOH, methanol (CH<sub>3</sub>OH), methane (CH<sub>4</sub>), formaldehyde (HCHO), and C<sub>2+</sub> products, such as C<sub>2</sub>H<sub>4</sub>, ethanol (C<sub>2</sub>H<sub>5</sub>OH), ethane (C<sub>2</sub>H<sub>6</sub>), acetic acid (CH<sub>3</sub>COOH), propanol (C<sub>3</sub>H<sub>7</sub>OH), among others (table 1). C<sub>2+</sub> products, characterized by higher energy densities and enhanced economic value, pose greater challenges in synthesis compared to C<sub>1</sub> products due to the increased number of protons and electrons requirement during conversion. Additionally, the elevated formation energy of C–C bonds can diminish reaction efficiency. The design and synthesis of high-performance electrocatalysts for eCO<sub>2</sub>RR are imperative to achieve specific product selectivity.

In the domain of CO<sub>2</sub> reduction studies, a thorough understanding of the underlying reaction mechanisms is crucial for advancing electrocatalytic processes. Central to this pursuit are several key topics, including elucidating reaction pathways,<sup>[36,37]</sup> identifying intermediates, discerning the roles of adsorbed CO, evaluating the impact of catalyst structure, and assessing the influence of electrolyte composition.<sup>[38–41]</sup> To explore into these intricate mechanisms, researchers employ a combination of experimental investigations and computational simulations. Computational simulations, in particular, offer a powerful tool for replicating experimental conditions and probing reaction kinetics at a molecular level.<sup>[42–44]</sup> In the field of quantum chemistry calculations, researchers scrutinize the electronic structure and energetics of chemical species to unravel the factors that govern catalytic performance. In particular, density functional theory (DFT) stands out for its overall accuracy and computational cost in the modelling of adsorption energies of reaction intermediates and energy barriers.<sup>[36,37,45]</sup> By leveraging DFT simulations, researchers can elucidate reaction pathways, assess the feasibility of catalytic processes, and guide the design of cost-effective materials with improved performance.<sup>[46]</sup> It is noteworthy that eCO<sub>2</sub>RR products exhibit significant variability, influenced by factors such as the electrocatalyst composition and morphology, electrolyte, and pH.<sup>[24,38,42,47]</sup> This variability underscores the complexity of the eCO<sub>2</sub>RR and the importance of comprehensive mechanistic studies in guiding the design of

**Table 1.** Standard reduction potentials for eCO<sub>2</sub>RR into different products in different reaction media.<sup>[31,35]</sup>

Electrolyte/ Products	Acid		Neutral		Base	
	Equation	E (V) vs RHE	Equation	E (V) vs RHE	Equation	E (V) vs RHE
Hydrogen	$2\text{H}^+ + 2\text{e}^- \rightarrow \text{H}_2$	0	$2\text{H}^+ + 2\text{e}^- \rightarrow \text{H}_2$	0	$2\text{H}_2\text{O} + 2\text{e}^- \rightarrow \text{H}_2 + 2\text{OH}^-$	-0.828
Formic acid/ formate	$\text{CO}_2 + 2\text{H}^+ + 2\text{e}^- \rightarrow \text{HCOOH}$	-0.171	$\text{CO}_2 + 2\text{H}^+ + 2\text{e}^- \rightarrow \text{HCOOH}$	-0.250	$\text{CO}_2 + \text{H}_2\text{O} + 2\text{e}^- \rightarrow \text{HCOO}^- + \text{OH}^-$	-0.639
Carbon monoxide	$\text{CO}_2 + 2\text{H}^+ + 2\text{e}^- \rightarrow \text{CO} + \text{H}_2\text{O}$	-0.104	$\text{CO}_2 + 2\text{H}^+ + 2\text{e}^- \rightarrow \text{CO} + \text{H}_2\text{O}$	-0.106	$\text{CO}_2 + \text{H}_2\text{O} + 2\text{e}^- \rightarrow \text{CO} + 2\text{OH}^-$	-0.932
Methane	$\text{CO}_2 + 8\text{H}^+ + 8\text{e}^- \rightarrow \text{CH}_4 + 2\text{H}_2\text{O}$	0.169	$\text{CO}_2 + 8\text{H}^+ + 8\text{e}^- \rightarrow \text{CH}_4 + 2\text{H}_2\text{O}$	0.169	$\text{CO}_2 + 6\text{H}_2\text{O} + 8\text{e}^- \rightarrow \text{CH}_4 + 8\text{OH}^-$	-0.659
Methanol	$\text{CO}_2 + 6\text{H}^+ + 6\text{e}^- \rightarrow \text{CH}_3\text{OH} + \text{H}_2\text{O}$	0.016	$\text{CO}_2 + 6\text{H}^+ + 6\text{e}^- \rightarrow \text{CH}_3\text{OH} + \text{H}_2\text{O}$	0.016	$\text{CO}_2 + 5\text{H}_2\text{O} + 6\text{e}^- \rightarrow \text{CH}_3\text{OH} + 6\text{OH}^-$	-0.812
Ethylene	$2\text{CO}_2 + 12\text{H}^+ + 12\text{e}^- \rightarrow \text{C}_2\text{H}_4 + 4\text{H}_2\text{O}$	0.085	$2\text{CO}_2 + 12\text{H}^+ + 12\text{e}^- \rightarrow \text{C}_2\text{H}_4 + 4\text{H}_2\text{O}$	0.064	$2\text{CO}_2 + 8\text{H}_2\text{O} + 12\text{e}^- \rightarrow \text{C}_2\text{H}_4 + 12\text{OH}^-$	-0.743
Ethane	$2\text{CO}_2 + 14\text{H}^+ + 14\text{e}^- \rightarrow \text{C}_2\text{H}_6 + 4\text{H}_2\text{O}$	0.144	$2\text{CO}_2 + 14\text{H}^+ + 14\text{e}^- \rightarrow \text{C}_2\text{H}_6 + 4\text{H}_2\text{O}$	0.144	$2\text{CO}_2 + 10\text{H}_2\text{O} + 14\text{e}^- \rightarrow \text{C}_2\text{H}_6 + 14\text{OH}^-$	-0.685
Ethanol	$2\text{CO}_2 + 12\text{H}^+ + 12\text{e}^- \rightarrow \text{CH}_3\text{CH}_2\text{OH} + 3\text{H}_2\text{O}$	0.084	$2\text{CO}_2 + 12\text{H}^+ + 12\text{e}^- \rightarrow \text{CH}_3\text{CH}_2\text{OH} + \text{H}_2\text{O}$	0.084	$2\text{CO}_2 + 9\text{H}_2\text{O} + 12\text{e}^- \rightarrow \text{CH}_3\text{CH}_2\text{OH} + 12\text{OH}^-$	-0.744
Acetic acid/ acetate	$2\text{CO}_2 + 8\text{H}^+ + 8\text{e}^- \rightarrow \text{CH}_3\text{COOH} + 2\text{H}_2\text{O}$	0.098	$2\text{CO}_2 + 8\text{H}^+ + 8\text{e}^- \rightarrow \text{CH}_3\text{COOH} + \text{H}_2\text{O}$	0.114	$2\text{CO}_2 + 5\text{H}_2\text{O} + 8\text{e}^- \rightarrow \text{CH}_3\text{COO}^- + 7\text{OH}^-$	-0.653
n-Propanol	$3\text{CO}_2 + 18\text{H}^+ + 18\text{e}^- \rightarrow \text{CH}_3\text{CH}_2\text{CH}_2\text{OH} + 5\text{H}_2\text{O}$	0.095	$3\text{CO}_2 + 18\text{H}^+ + 18\text{e}^- \rightarrow \text{C}_3\text{H}_7\text{OH} + \text{H}_2\text{O}$	0.104	$3\text{CO}_2 + 13\text{H}_2\text{O} + 18\text{e}^- \rightarrow \text{CH}_3\text{CH}_2\text{CH}_2\text{OH} + 18\text{OH}^-$	-0.733

more efficient and selective electrocatalysts for sustainable carbon utilization.

Despite the potential to generate a range of products, attaining precise selectivity towards a specific outcome remains a significant challenge. This difficulty primarily stems from the able closely matched thermodynamic standard reduction potentials among various CO<sub>2</sub> reaction pathways, which limits selectivity towards the desired product. The challenge extends beyond the multiple electron and proton transfer processes; it is also about achieving a delicate balance to navigate the thermodynamic landscape for targeted product yields. The catalyst effectiveness is therefore paramount, as it overcomes the energy barriers associated with these multi-step electron transfer steps. Effective design expedites the formation of intermediates, enhances the selectivity of the desired product, and minimizes side or competing reactions, thus reducing energy demands and improving selectivity. In summary, while eCO<sub>2</sub>RR holds promise for sustainable production, attaining high selectivity requires a profound understanding of the complex factors that govern this process. Ongoing research efforts are diligently directed toward unravelling these complexities and developing innovative strategies to increase selectivity in this pivotal process.

## 2.2. Economic Analysis and Industrial Perspective of eCO<sub>2</sub>RR Products

From an industrial perspective, eCO<sub>2</sub>RR involves developing electrocatalytic technologies and catalysts to convert carbon dioxide into economically viable, valuable products at a pilot

scale. Currently, the industrial scenario for eCO<sub>2</sub>RR lags that of water electrolysis, although a direct comparison is challenging due to the complex nature of reactions involved in both processes. However, significant progress has been made in commercializing specific products like HCOOH and CO from eCO<sub>2</sub>RR.<sup>[48]</sup> In contrast, the development of C<sub>2+</sub> products, such as ethylene and ethanol, remains in a significant development phase. One major commercialization challenge is identifying critical aspects of fundamental reactions.<sup>[48]</sup> Other challenges involve scaling up and translating promising lab-scale results to larger scales. For example, reproducibility issues may arise from using different setups in tests and overlooking hidden variables during material and GDEs preparation. These variables include considerations like stopping the reaction to take samples, system cleaning steps, real-time monitoring, using an inert gas stream for accurate CO gas analysis, and measuring CO<sub>2</sub> on both the anodic and cathodic sides of the cell to understand product crossover. Sharing detailed information about the properties and structure of electrodes is also crucial. To tackle these issues, establishing specific plans and guidelines for each electrocatalyst's preparation, electrode and GDE production, and testing process is essential. A comprehensive analysis and development of electrocatalysts with scalable, reproducible technology is vital for creating a supportive ecosystem for eCO<sub>2</sub>RR. Therefore, we identify five key areas essential for successful collaboration to achieve industrial targets for eCO<sub>2</sub>RR: Fundamental electrochemical analysis, Catalyst material development, Statistic, Engineering, Economic viability (figure 1).

The market for products derived from eCO<sub>2</sub>RR is still nascent and varies based on specific products and their applications. Influenced by factors such as technological advancements,

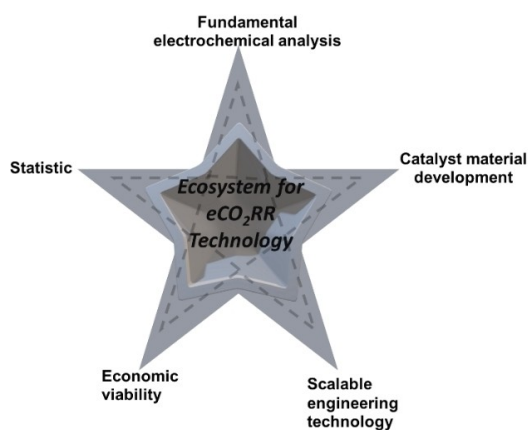


**Figure 1.** Illustration of five key points for the development of an eCO<sub>2</sub>RR technology ecosystem.

regulatory frameworks, and investment in sustainable solutions, the market is steadily growing. However, precise market size figures are difficult to determine due to the diversity of products and the evolving nature of the industry. Despite these challenges, there is a growing interest and investment in CO<sub>2</sub> utilization technologies, driven by the imperative to address climate change, market pull for sustainably produced products and achieving carbon neutrality goals. These products find applications across various sectors, including renewable energy, transportation, and chemical manufacturing. Driven by the advancements in research and development and increasing commercialization, the market for eCO<sub>2</sub>RR products is expected to see significant growth in the coming years.<sup>[49]</sup> Industry analysts and market research firms may offer more up-to-date and detailed information on market sizes and growth projections for these technologies.<sup>[49,50]</sup> For instance, our view of recent articles revealed varied production volumes and applications for these products, as illustrated in Figure 2a. Although hydrogen is a side product of eCO<sub>2</sub>RR, it is highlighted for price

comparisons due to its usefulness as a fuel. Notably, ethylene and ethanol are highlighted as having considerably larger markets compared to other products, depending on the applications,<sup>[48]</sup> as shown in Figure 2b.

The current landscape of carbon capture and utilization (CCU) technologies reveals that electrochemical conversion of CO<sub>2</sub> into chemicals accounts for a significant 25% share (Figure 3). Since the database is currently populated by projects mainly from Europe, the data in Figure 3B is skewed towards EU projects. A detailed assessment using TRL indicates that many of these technologies are in the development or demonstration phases (Table S1). Techno-economic assessment (TEA) is a critical methodology for evaluating the economic viability of technologies or processes. By assessing both technological performance and economic feasibility, TEA identifies key parameters that determine economic viability, thereby informing decisions about continuing or halting research, development, and investment activities.

In the context of CO<sub>2</sub> reduction technologies, TEA has been pivotal in evaluating commercial potential and identifying areas needing improvement. Various studies have explored the TEA of low-temperature CO<sub>2</sub> electrolysis, focusing on the production of renewable chemicals and fuels like carbon monoxide, formic acid, ethylene, and ethanol. These studies have shed light on production costs, showing that carbon monoxide and formic acid are cost-competitive, while the production of ethylene and ethanol faces economic feasibility challenges due to higher costs. Furthermore, TEA has guided technological advancement and provided guidelines for market deployment. Although low-temperature CO<sub>2</sub> electrolysis has been recognized for its potential to generate renewable chemicals and fuels, challenges persist. These include the lack of comprehensive roadmaps, the need for interdisciplinary approaches, and the consideration of variable operational schedules and market prices. Addressing these issues requires continued research and interdisciplinary collaboration.

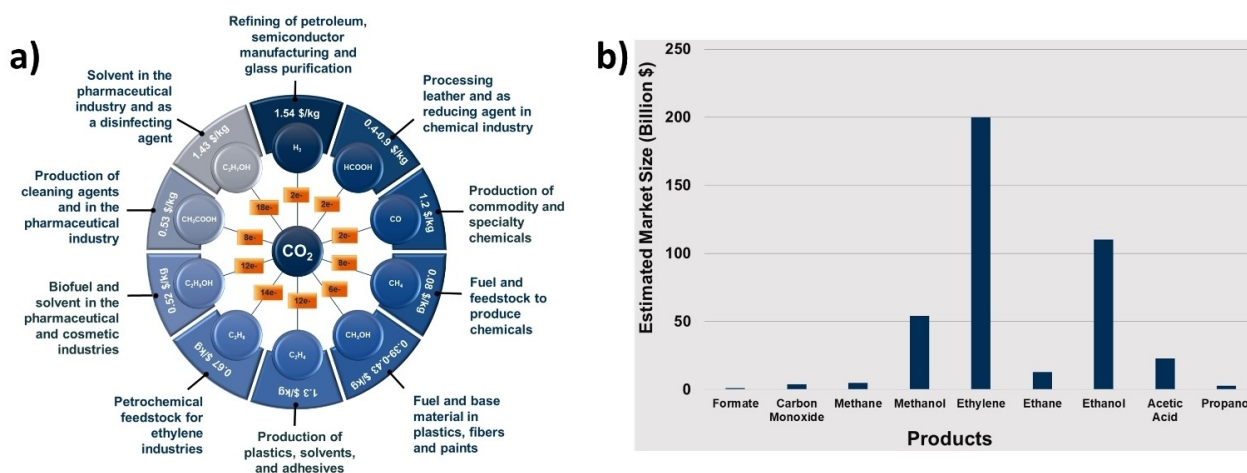


**Figure 2.** a) A schematic illustrating the various products that can be generated via eCO<sub>2</sub>RR, alongside their respective applications and market prices in \$/kg. This diagram provides a visual overview of the potential commercial value and utility of each product derived from eCO<sub>2</sub>RR. b) A bar graph depicting the estimated market size for these products in the past decade, offering a comparative perspective on their economic impact within the industry.<sup>[51-53]</sup>

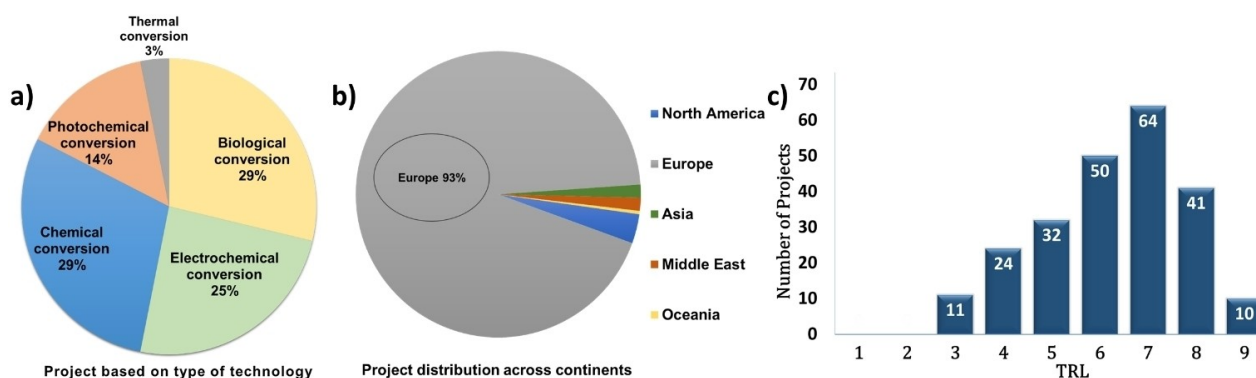


**Figure 3.** a) Pie chart detailing the proportion of carbon capture and utilization projects (in Europe), delineating their scope and status. b) Chart highlighting the global distribution of carbon capture and utilization projects, illustrating the international engagement in carbon conversion technology. c) Bar chart displaying the carbon capture and utilization projects according to their TRLs, offering an overview of project maturity and readiness for commercial deployment.\*\* The figures are based on the CCU projects database prepared by CO2ValueEurope (available at <https://database.co2value.eu/>)

Numerous publications have addressed the essential criteria for advancing technologies to commercial viability. Notably, Seget et al.<sup>[17]</sup> provided a comprehensive analysis of the pivotal parameters and challenges for commercializing the process. They juxtaposed the state-of-the-art performances against these key performance parameters, offering an in-depth comparison and addressing the practical challenges encountered in industrial applications as shown in Table 2. The parameters identified by Seget and co-workers serve as valuable benchmarks for assessing the readiness of a technology for the marketplace.

### 2.3. eCO<sub>2</sub>RR Reactor Types and Operational Parameters

The efficiency and selectivity of eCO<sub>2</sub>RR are significantly influenced by the design of the reactor and its operational parameters, which are pivotal in determining the production of specific chemicals. There are several classifications of eCO<sub>2</sub>RR reactors, detailed in Figures 4 and 5, each with its own advantages and characteristics:

#### 2.3.1. Batch Reactors

In batch reactors, a CO<sub>2</sub>-saturated electrolyte is contained within a sealed vessel where electrochemical reactions are conducted under precise conditions. Batch reactors are favored for initial screening of catalysts and reaction conditions due to their simplicity and straightforward operation. One common example of this type of reactor is the H-type cell. Despite their operational ease, these reactors often suffer from mass transport limitations and low productivity compared to flow reactors.

**Operational Parameters:** Factors critical to batch reactor performance include the composition of the electrolyte (affecting CO<sub>2</sub> solubility and ion mobility), electrode material, catalyst loading, as well as temperature, pressure, stirring rate, and reaction time.

**Advantages:** Batch reactors are valued for their simplicity and ease of operation. They allow for controlled testing environments conducive to detailed analysis of reaction mechanisms and catalyst efficiencies. Their adaptability in modifying

**Table 2.** Comparison of the minimum requirements for industrial applications with the current state-of-the-art for various eCO<sub>2</sub>RR products, including CO, HCOOH, and C<sub>2</sub>H<sub>4</sub>. Data adapted from Ref. [17].

Entry	Key performance parameters	State-of-the-art
Current density	> 0.2 A cm <sup>-2</sup>	0.5–1.8 A cm <sup>-2</sup>
Energy efficiency	> 50 %	ca. 40 %
Faradaic efficiency	> 80 %	80–90 %
Full cell potential @ 300 mA cm <sup>-2</sup>	< 3.0 V, better < 2.5 V, ideally < 2.0 V	2.7 V
System temperature	60–90 °C	40–80 °C
Single pass conversion	> 50 %	30–70 %
<b>Additional notes and Challenges</b>		
Stability	< 10 μVh	
Cost of electricity	< 0.04 \$ kWh	
Carbon balance	Use of internal standards – Quantification of the anode gas stream	
Membranes of choice	Anion exchange membranes (AEMs) – more energy efficient bipolar membranes (BPMs) are required	
Purity of substrates	Minimum vol % of CO <sub>2</sub> in gas-stream – ca. 10 % and minimization of NO <sub>x</sub> and O <sub>2</sub> impurities	

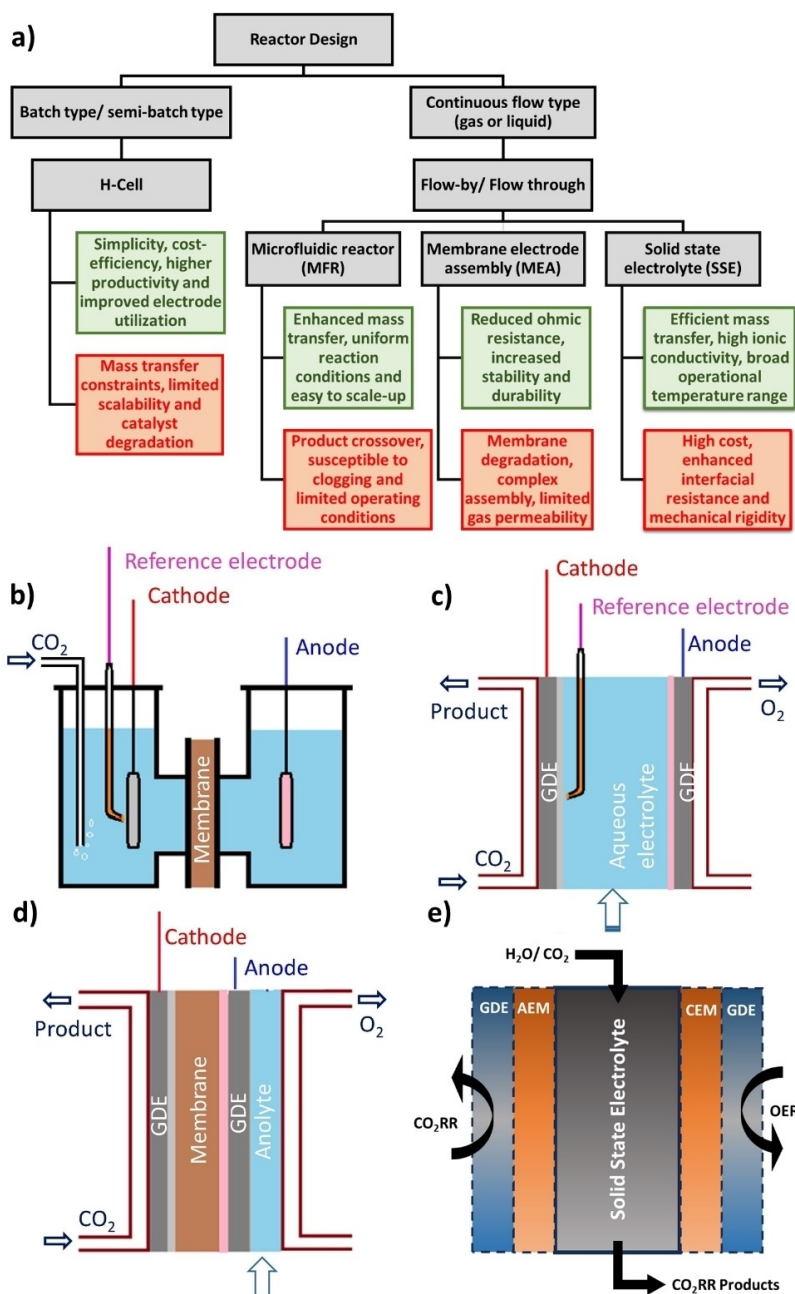


**Figure 4.** a) Classification of reactor designs along with their advantages (green text) and disadvantages (red text). Schematic representation of H-cell. (b), microfluidic cell (c), MEA setup (d), SSE reactor (e). Figure 4b, c, d Reproduced with permission<sup>[54]</sup> Copyright 2020, Elsevier.

operational conditions make them suitable for catalyst screening studies.

### 2.3.2. Flow Reactors

Flow reactors function as continuous-flow systems where a  $\text{CO}_2$ -saturated electrolyte or gas passes through an electrochemical cell. They allow for precise control of various reaction conditions like flow rate, temperature, and pressure, which leads to more efficient mass transport and potentially enhanced selectivity. These reactors are versatile, scalable from small laboratory

setups to larger industrial applications. Flow reactors are further subdivided into microfluidic (MFR), membrane electrode assembly (MEA), and solid-state electrolyte (SSR) reactors.

#### 2.3.2.1 Microfluidic Reactors

Microfluidic reactors, (Figure 4) also known as microreactors, are miniaturized systems with reaction volumes ranging from a few microliters to milliliters. These compact devices are designed to enhance reaction performance through features such as high surface area-to-volume ratios, rapid mixing, and enhanced mass

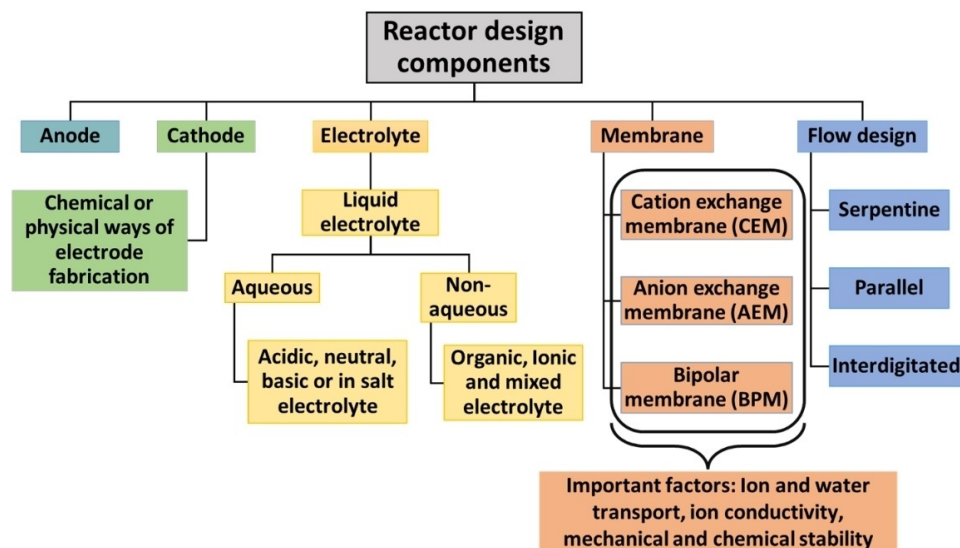


Figure 5. Classification of reactor components used for eCO<sub>2</sub>RR.

transport. Consequently, these characteristics lead to more efficient reaction kinetics and improved product selectivity. Microreactors are especially beneficial for high-throughput experiments, enabling rapid screening of catalysts and varied reaction conditions.

**Operational Parameters:** Flow rate, reaction volume, electrode material, catalyst loading, temperature, pressure, and residence time.

**Advantages:** The small-scale setup allows for high-throughput screening capabilities and reduced reagent use, which can lower costs. Other benefits include enhanced reaction kinetics due to improved mass transport, the potential for system integration, and overall cost-effectiveness due to lower material requirements.

**Disadvantages:** Despite these advantages, microfluidic reactors can encounter issues such as product crossover, which may lead to reoxidation and efficiency losses. Additionally, the compact design can lead to flooding, where the electrolyte fills the reaction channels and disrupts gas flow, further affecting the reaction efficiency.

### 2.3.2.2. Membrane Electrode Assemblies (MEA)

MEA-based reactors (Figure 4) feature ion-exchange membranes to separate the anode and cathode compartments. This design allows for the selective transport of ions and reduces the crossover of reactants and products, thereby enhancing the reactor's efficiency. The careful optimization of the electrode-membrane interface in MEA reactors is crucial, as it plays a key role in the efficient mass transport of reagents and the selectivity of the eCO<sub>2</sub>RR process.

**Operational Parameters:** Factors critical to MEA performance include the type of ion-exchange membrane used, electrode material, catalyst loading, composition of the electrolyte,

temperature, pressure, and current density applied across the cell.

**Advantages:** MEA reactors are known for their enhanced selectivity and ability to minimize crossover effects. They also support improved mass transport and can be arranged in stack configurations for scalability. Additionally, these systems offer reduced electrical impedance and are less prone to flooding.

**Disadvantages:** Despite their efficiency, MEA reactors may not be the most suitable option to produce liquid products. They can experience issues such as carbonate precipitation, which can impact long-term operation and efficiency. Furthermore, although less prone to flooding, they are not entirely immune, especially when dealing with high electrolyte volumes.

### 2.3.2.3. Solid-State Electrolyte (SSE)

SSE reactors (Figure 4) for eCO<sub>2</sub>RR utilize a solid-state electrolyte membrane strategically positioned between two electrode compartments. This electrolyte functions as a medium for ion transport, specifically oxygen or carbonate ions, facilitating electrochemical reactions while ensuring gases and liquids do not mix. The solid nature of the electrolyte not only aids in ion conduction but also maintains the mechanical integrity essential for efficient operation. Typically, the electrodes in SSE reactors are made of catalyst materials supported on conductive substrates like carbon or metal foils.

**Operational Parameters:** Critical factors for SSE performance encompass the electrolyte material, operating temperature, gas composition, flow rate, applied potential and current density, catalyst loading and composition, electrode configuration and geometry, and reactant concentration.

**Advantages:** SSE reactors are notable for their safety and stability, with the solid electrolyte reducing risks of leaks and side reactions. They offer high ionic conductivity, essential for

efficient charge transport, and are designed to be flexible for integration into different systems. The durability and potential scalability make SSE reactors attractive for large-scale applications.

**Disadvantages:** While SSE reactors offer numerous benefits, they also face some challenges. These include higher upfront costs due to more expensive materials and complex manufacturing requirements. Increased internal resistance (IR losses) can also diminish energy efficiency. Furthermore, maintenance and replacement of solid electrolytes can be more cumbersome compared to systems using liquid electrolytes, posing additional operational challenges.

Understanding the role of each component within eCO<sub>2</sub>RR reactors is essential for optimizing reactor design and enhancing performance. In the following we outline the primary components (Figure 5) found in eCO<sub>2</sub>RR reactors:

### 1. Electrodes

**Cathode:** The cathode is the electrode where CO<sub>2</sub> reduction reactions take place and is typically composed of conductive materials such as metals or carbon-based structures. GDE are commonly used, especially in industrial settings, due to their porous structure (often carbon paper or cloth) that facilitates CO<sub>2</sub> transport to the catalyst-coated surface. This arrangement enhances the reduction of CO<sub>2</sub> to products like hydrocarbons or oxygenates, addressing challenges related to mass transport, reaction kinetics, and catalyst stability.

- Anode:** The anode facilitates oxidation reactions like the oxygen evolution or alcohol oxidation reactions required to maintain charge balance within the electrochemical cell and is constructed from oxidation-resistant materials.
- Catalysts:** Catalysts are crucial for promoting CO<sub>2</sub> reduction, enhancing selectivity, and improving efficiency. They expedite CO<sub>2</sub> adsorption, activation, and conversion to the desired products. Catalysts may be supported on or integrated into the electrode material, with common choices including transition metals (e.g., copper, silver, gold), metal alloys, metal oxides, and heteroatom-doped carbon materials.
- Electrolyte:** The electrolyte acts as the ion transport medium between the cathode and anode, providing conductivity and setting the reaction's chemical environment. Typical electrolytes in eCO<sub>2</sub>RR include aqueous solutions containing salts like potassium bicarbonate (KHCO<sub>3</sub>), potassium hydroxide

(KOH), or acidic solutions such as sulfuric acid (H<sub>2</sub>SO<sub>4</sub>). Non-aqueous electrolytes are also used in specific setups to tailor the reaction conditions<sup>[55]</sup> (Table 3). Selection of electrolyte is always very important as each of the electrolyte has advantages and disadvantages over each other.

- Ionic Conductive Membranes:** Membranes play a crucial role in enhancing the efficiency and selectivity of eCO<sub>2</sub>RR by facilitating reactant and product transport while minimizing side reactions. Types of membranes include proton/cation exchange membranes (PEM/CEM), anion exchange membranes (AEM), and bipolar membranes (BPM), which facilitate the selective transport of protons, anions, and both, respectively. Their performance is influenced by factors such as membrane strength, thickness, temperature, humidity, pressure, and chemical compatibility, necessitating thorough optimization.
- Gas Distribution System:** This system is designed to deliver CO<sub>2</sub> efficiently to the cathode surface. It includes components like flow lines and gas distribution channels within the reactor's current collector. Various flow designs (e.g., serpentine, parallel, interdigitated) offer unique properties that cater to different eCO<sub>2</sub>RR requirements.

## 3. eCO<sub>2</sub>RR Products Current Trends

### 3.1. CO

Carbon monoxide, the simplest carbon oxide, is a colorless, odorless, and tasteless flammable gas with diverse applications. It serves as a chemical feedstock in large-scale industrial processes such as Fischer-Tropsch (FT) synthesis, water gas shift reaction, pharmaceutical manufacturing, and methanol synthesis.<sup>[56,57]</sup> In the steel and metals industries, CO is used as a reducing agent for metal extraction from ores. Furthermore, CO, in conjunction with methanol, undergoes the Cativa process using an iridium-based catalyst to produce acetic acid, the predominant method for industrial acetic acid synthesis.<sup>[56-58]</sup> CO offers an energy-efficient pathway for industrial processes as it is employed in cogeneration systems which effectively produce both electrical and thermal energy.

CO is naturally emitted to the atmosphere through biological processes and volcanic eruptions, alongside anthropo-

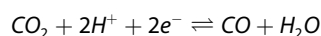
**Table 3.** Comparison between alkaline, acidic, neutral, pure water and non-aqueous electrolytes.

Electrolyte Type	pH Range	Advantages	Challenges
Alkaline	10–14	High efficiencies, better product selectivity, improved CO <sub>2</sub> solubility, suppress HER.	Salt formation leads to low carbon conversion efficiencies, highly chemically corrosive.
Acidic	0–4	High CO <sub>2</sub> solubility, fast kinetics, minimal salt formation.	Competing HER leading to low faradaic efficiency, limited selectivity for C2 products.
Neutral	~7	Moderate CO <sub>2</sub> solubility, minimal CO <sub>2</sub> losses, avoids the corrosion of materials, low salt precipitation.	Sluggish reaction kinetics, higher potentials, low product selectivity.
Pure Water	~7	Clean sustainable solution, low cost, easy downstream process.	Low conductivity, higher overpotentials.
Non-aqueous	varies	High CO <sub>2</sub> solubility, reduced side reactions.	Solvent stability, complex reaction mechanisms, low current densities.

genic sources like partial combustion and industrial activities. These include partial oxidation of carbon-containing compounds, and reforming of hydrocarbon-rich feedstocks such as coal, natural gas, and mineral oil fractions. The conventional industrial production of CO, however, poses significant environmental challenges, particularly regarding sustainability and greenhouse gas emissions. To mitigate these impacts, there is a pressing need to adopt greener and more sustainable production techniques.

The electrochemical conversion of CO<sub>2</sub> to CO offers a carbon-neutral solution that is economically viable and could potentially replace fossil-fuel-based methods.<sup>[59]</sup> This process, involving the transfer of two electrons/protons, is one of the simplest transformations that can be achieved through eCO<sub>2</sub>RR. Additionally, because CO is a gas, the costs associated with its separation from aqueous electrolytes are significantly reduced. However, for CO<sub>2</sub> electrolyzers to be commercially viable, they must produce CO at an industrially significant rate (5–10 t<sub>CO</sub> h<sup>-1</sup>) to compete with fossil fuel processes.<sup>[60]</sup>

Substantial research is being conducted to develop robust CO<sub>2</sub> electrolyzers capable of meeting industrial demands (Table S2). The success of these reactors in the market largely depends on achieving high chemical output rates or throughput, which in turn relies on the activity and durability of the electrocatalyst used.<sup>[60]</sup> The electrochemical conversion of CO<sub>2</sub> to CO, shown in Eq. (1), involves multiple steps, namely adsorption, activation, reduction and desorption.



This reaction takes place in an electrochemical cell where CO<sub>2</sub> is introduced at the cathode, and the process is facilitated by a suitable electrolyte and electrode, typically involving metal catalysts. The reaction pathway can vary depending on factors such as catalyst material, electrode potential, electrolyte composition, and overall reaction condition.<sup>[61]</sup> Some intermediates that may form during the reaction include carbonate, bicarbonate, carboxylate, and formate. These intermediates influence the selectivity, efficiency, and kinetics of CO<sub>2</sub> conversion to CO.

Understanding the formation and behavior of these intermediates is essential for optimizing catalyst design and reaction conditions to enhance the desired CO production while minimizing unwanted byproducts. For instance, optimal catalysts typically exhibit a significant binding energy for the \*COOH intermediate and a weak binding energy for CO to ensure selective CO production. Additionally, the catalyst should display a weak binding affinity for H atoms, resulting in an unfavorable thermodynamic environment for the competing hydrogen evolution reaction (HER) in aqueous solutions.

### 3.1.1. Catalysts

In 1993, Hori et al. classified different monometallic electrodes based on the primary eCO<sub>2</sub>RR products, identifying gold (Au),

silver (Ag), and zinc (Zn) as electrocatalysts for the selective conversion of CO<sub>2</sub> to CO.<sup>[61,62]</sup>

#### 3.1.1.1. Au-Based Catalysts

Gold is well-documented for its exceptional activity and selectivity in converting CO<sub>2</sub> to CO at low overpotentials, positioned near the peak of the kinetic volcano plot for CO formation.<sup>[63]</sup> The influences of size,<sup>[64]</sup> composition,<sup>[65,66]</sup> morphology,<sup>[67]</sup> and reaction kinetics on its performance have been extensively studied. For instance, Varo et al. explored the effect of nanoparticle size on selectivity during CO<sub>2</sub> electroreduction, finding that gold nanoparticles around 3 nm maximize selectivity towards CO with Faradaic efficiencies (FEs) reaching up to 60% at relatively low potentials.<sup>[64]</sup> Studies have also investigated the nanostructuring of Au-based materials, showing that configurations like nanoclusters,<sup>[68]</sup> nanowires,<sup>[67]</sup> and nanoneedles<sup>[69]</sup> enhance CO selectivity and catalytic activity. Kim et al. demonstrated that Au nanostructures have higher CO selectivity at lower overpotentials than untreated Au films, resulting in faster stabilization of the CO<sub>2</sub><sup>-</sup> intermediate. In particular, at an overpotential of 280 mV, pore-like structures showed higher CO selectivity than pillar-like structures, although the latter demonstrated greater selectivity and current density at higher overpotentials.<sup>[70]</sup> Furthermore, enhancing the intrinsic activity of Au through the incorporation of a secondary metal via alloying, intercalation, and core-shell structuring has been shown to improve mass transport and reaction kinetics.<sup>[71]</sup> Despite their high efficiency, the broader application of gold-based catalysts in large-scale processes is hindered by their cost.

#### 3.1.1.2. Ag-Based Catalysts

Silver-based catalysts present a less expensive alternative to gold, with significant effectiveness in the selective conversion of CO<sub>2</sub> to CO.<sup>[72]</sup> Rosen et al.'s pioneering work demonstrated the high efficiency of Ag nanoparticles, achieving FE of 96% for CO production.<sup>[73]</sup> The activity, stability, and selectivity of Ag catalysts can be similarly enhanced by modifying the active sites and introducing secondary metals. Chandrashekar et al.<sup>[74]</sup> explored AgPd alloys at industrial current densities (50 to 200 mA cm<sup>-2</sup>), finding that increasing the Pd content reduced selectivity from 99% with pure Ag to 73% with pure Pd at 50 mA cm<sup>-2</sup>. Notably, MEA configurations facilitated substantial CO current densities of 123 mA cm<sup>-2</sup>.<sup>[74]</sup> In another study, Park et al.<sup>[75]</sup> tested bimetallic Au–Ag nanostructures, achieving a CO current density of 95 mA cm<sup>-2</sup> with 88% FE at an applied cell potential of 2.75 V in MEA cells under neutral conditions. This study highlighted that adding a small amount of Au precursor can significantly enhance reaction kinetics and mass transport.

### 3.1.1.3. Zn-Based Catalysts

Zinc-based electrocatalysts stand out as a low-cost, earth-abundant alternative to noble metals,<sup>[72]</sup> exhibiting high selectivity for converting CO<sub>2</sub> to CO.<sup>[76]</sup> Luo et al.<sup>[77]</sup> developed a porous Zn electrode through a straightforward electrodeposition method to enhance both activity and CO selectivity. When tested in a flow-cell reactor and converted it into a GDE, this Zn electrode achieved an impressive current density of 200 mA cm<sup>-2</sup> and a FE of 84% for CO production at -0.64 V vs RHE.

In addition to pure Zn catalysts, the integration of Zn with other non-precious metals, such as Cu, has shown promising results. These bimetallic systems leverage the synergistic effects between the metals to enhance catalytic performance. Wang et al.<sup>[78]</sup> investigated a Zn-rich Zn–Cu electrocatalyst, noting substantial improvements in selectivity and activity for CO production compared to pure Zn and Cu catalysts. The bimetallic catalyst achieved a remarkable FE of 97%.<sup>[78]</sup> They also employed this Zn–Cu powder catalyst in a vapor-fed reactor with planar electrodes, confirming the effectiveness of GDEs in CO<sub>2</sub> to CO conversion under practical operating conditions. This study further emphasizes the pivotal role of synergistic effects in stabilizing the carboxyl intermediate, a key aspect in enhancing CO selectivity.

### 3.1.1.4. Hybrid Inorganic Metal-Based Catalysts

Hybrid inorganic metal-based catalysts represent a burgeoning class of catalysts for the selective conversion of CO<sub>2</sub> to CO. A notable development in this area is the work by Li and co-workers,<sup>[79]</sup> who utilized Cu@In<sub>2</sub>O<sub>3</sub> core-shell structures for syngas production. Their study demonstrated that varying the shell thickness of In<sub>2</sub>O<sub>3</sub> significantly affects catalyst performance, allowing for a wide range of H<sub>2</sub>:CO ratios from 4:1 to 0.4:1 and achieving FEs over 90%. The top-performing C–Cu/In<sub>2</sub>O<sub>3</sub> catalyst exhibited high activity, achieving an impressive current density of 4.6 mA cm<sup>-2</sup> at an overpotential of -0.6 V vs. RHE and 12.7 mA cm<sup>-2</sup> at -0.9 V vs. RHE, respectively.<sup>[80]</sup> Additionally, the role of carbon materials such as graphite, graphene, and carbon nanotubes, known for their unique electronic structures and ability to support metal nanoparticles, was highlighted, although these require further enhancements in selectivity and efficiency.<sup>[81]</sup> Hybrid catalysts that incorporate earth-abundant elements and other components like metal-organic frameworks (MOFs) also show promising synergistic effects, enhancing eCO<sub>2</sub>RR performance.<sup>[53,82,83]</sup> These developments suggest new research pathways for improving the efficiency and selectivity of eCO<sub>2</sub>RR processes.

### 3.1.2. Reactor

The most promising electrochemical reactor designs for large-scale commercialization of converting CO<sub>2</sub> to CO at ambient

room temperatures are the MEA Reactor and the Gas Phase Electrolyzer.<sup>[83]</sup>

The MEA reactor is particularly promising due to its compactness, ability to achieve high current densities and efficient mass transport. Its scalability and performance make it suitable for large-scale applications. Significant progress has been made in developing MEAs for industrial use under ambient conditions. For instance, Quentmeier et al. introduced a short-stack MEA design with three cells, which is advantageous for scaling up MEA configurations. Their research showed that at high current densities (300–400 mA cm<sup>-2</sup>), the short stack outperformed single-cell setups, with lower stack voltages and variable cell voltages depending on the cell's position within the stack.<sup>[84]</sup> This highlights the modular short-stack design as crucial for early evaluation and scaling of CO<sub>2</sub>-to-CO electrolysis for industrial applications. Kutz et al. demonstrated that anion-conductive membrane-based MEAs could operate stably for 4,380 hours with a 98% selectivity for CO production. These tests were carried out on a 5 cm<sup>2</sup> Ag electrode overcoming the challenges related to upscaling of electrode and the process.<sup>[85]</sup>

The gas phase electrolyzer, featuring separate chambers for CO<sub>2</sub> gas, catholyte, and anolyte, is also a promising design for efficient CO<sub>2</sub> conversion. This setup allows for effective CO<sub>2</sub> conversion and can be scaled up for commercial use.<sup>[51]</sup> Quentmeier et al. led a stepping stone towards upscaling the CO<sub>2</sub>-to-CO electrolyzer by developing a stackable cell capable of meeting industrially relevant conditions. Their study necessitated the creation of specialized media flow chambers. To achieve this, the gas chamber, which interfaces with the GDE from the anode's far side, was engineered to regulate the feed gas flow and distribution. Concurrently, an ionically conductive spacer was integrated into the catholyte chamber on the opposite side of the GDE, which influenced cell voltage, selectivity, and overall conversion efficiency. These modifications were shown to increase Faraday efficiency for CO, particularly under conditions of reduced CO<sub>2</sub> supply, by optimizing the feed gas distribution. The inclusion of the spacer also contributed to process stability by reducing fluctuations in cell voltage caused by gas bubbles. Collectively, these enhancements provided mechanical robustness and ensured consistent ionic and electric contact across the entire active cell area, which is essential for the stacking and upscaling of the cell.<sup>[84]</sup>

Both reactor designs excel in efficiency, scalability, and potential for high current densities, making them well-suited for large-scale commercialization of electrochemical CO<sub>2</sub> to CO conversion. The choice between these designs depends on factors like efficiency, scalability, and specific application requirements, as each has its own unique advantages and challenges.

### 3.2. Formic Acid

Formic acid (FA) is an organic acid finding widespread use across textile, pharmaceutical, feed, and agriculture sectors due to its environmentally friendly nature, non-corrosiveness, and

biodegradability.<sup>[86]</sup> Its utility extends beyond traditional industry roles, serving as a chemical reductant, green solvent, and a precursor in many chemical syntheses.<sup>[87]</sup> With an estimated global market projected to increase from US\$ 1.8 billion in 2023 to US\$ 2.8 billion by 2033, FA is anticipated to witness sustained growth.

Besides being a chemical commodity, the role of FA as energy carrier is gaining traction due to its potential in addressing energy storage challenges. Its capacity for direct production or upgrading into fuels such as H<sub>2</sub>, CO, methanol, and bio-oils, particularly with a volumetric capacity of 53.4 g/L or 4.4 wt% of H<sub>2</sub>, aligns with the US Department of Energy's target of value of 5.5 wt% for effective H<sub>2</sub> storage.<sup>[62,88]</sup>

FA's capability as an energy carrier is also valuable for gaseous fuels, simplifying storage and transport challenges in practical applications. Its dehydrogenation to H<sub>2</sub> is simple, mild, and easily controllable, making FA a potential CO storage material as well. These properties underscore FA's significance to both the chemical industry and energy sectors.<sup>[89]</sup>

Currently, FA's production in Europe predominantly employs chemical synthesis routes, such as the catalytic hydrogenation of CO or the hydrolysis of methyl formate derived from methanol and CO in the presence of a strong base.<sup>[89]</sup> Microbial fermentation processes present sustainable alternatives, leveraging the natural or engineered metabolic pathways of certain bacteria and fungi that produce FA as a byproduct.<sup>[90]</sup>

However, the eCO<sub>2</sub>RR to FA is a versatile avenue in the field of sustainable chemistry and carbon capture technologies. This process not only aligns with the global drive towards sustainability by utilizing renewable energy sources, but it also presents the potential for direct application without the necessity for purification. This aspect streamlines the downstream processing, thereby mitigating the overall production expenditure.<sup>[2,91]</sup>

Following are the primary advantages of eCO<sub>2</sub>RR to FA that drives extensive research and process modification:

1. Renewable energy integration: Harnessing renewable electricity from sources such as solar or wind power.
2. Selective production: High selectivity towards FA production with minimal undesired products.
3. High efficiency: Electrochemical methods can be highly efficient in converting CO<sub>2</sub> to FA.
4. Modularity and scalability: The process can be tailored and scaled to meet demand flexibly.
5. Reduced environmental impact: Lower emissions and reduced chemical waste.
6. Potential for direct utilization without purification: Simplifying downstream processing and reducing costs.

Electrochemical routes for FA production are undergoing extensive research to refine and optimize these advantages for industrial application, paving the way for a more economically viable synthesis of FA (Table S3).

### 3.2.1. Catalyst Design

The eCO<sub>2</sub>RR to formate has been a focal point of research since the pioneering work of Hori et al.<sup>[92]</sup> Advances over the years have led to notable improvements in catalyst selectivity,<sup>[93]</sup> particularly with metals such as Sn, Bi, Pb, and In, which are known to favor the formation of formate through the eCO<sub>2</sub>RR.<sup>[94]</sup> While the efficiency of Sn as a catalyst has been widely documented,<sup>[92,93,95]</sup> challenges regarding the long-term stability of such catalysts have prompted further innovation.<sup>[96]</sup>

To address stability issues, researchers have employed a variety of strategies, focusing primarily on catalyst development. These approaches include modifying catalyst surface morphology through diverse synthesis methods,<sup>[97–99]</sup> doping with heteroatoms to bolster stability,<sup>[121]</sup> and preventing the agglomeration of active metal sites. Bimetallic systems have been created using alloying techniques or by the introduction of trace amounts of dopant heteroatoms, with some modifications yielding significant enhancements in both stability and selectivity for converting CO<sub>2</sub> to formate.<sup>[71]</sup>

The eCO<sub>2</sub>RR to FA involves a series of steps at the electrode surface, namely adsorption, activation, reduction, protonation, and release of the product into the solution or gas phase. The possible reaction pathways are marked by the intermediates CO<sub>2</sub><sup>-</sup>, \*COOH, and CHO<sup>-</sup> making the stabilization of the \*OCHO intermediate a key focus in catalyst design, while impeding the competing HER and the formation of other potential eCO<sub>2</sub>RR products like CO.<sup>[100]</sup>

A notable study by Laing et al. highlighted the efficacy of S-doped Cu<sub>2</sub>O, where sulfur adsorption on reduced Cu<sub>2</sub>O creates active sites that favor the adsorption of \*OCHO, thus diminishing the competing HER and CO pathways.<sup>[101]</sup> It was found that S-adsorbed Cu(111) surfaces possess a higher energy barrier for the formation of the \*COOH intermediate compared to bare Cu(111), reducing the likelihood of CO<sub>2</sub> being converted to CO. In line with these findings, Chen et al. reported on the use of Bi–In nanotubes which, following a similar rationale, achieved a partial current density of 1.03 A cm<sup>-2</sup> with a FE of 95.3% and maintained stability for 48 h in an MEA cell configuration.<sup>[102]</sup> In-situ reconstruction of Bi<sub>60</sub>In<sub>2</sub>O<sub>93</sub> nanotube for stable eCO<sub>2</sub>RR electroreduction of CO<sub>2</sub> at ampere-current densities. Another example is S–Sn, where S doping was deemed to stabilize the \*OCHO intermediate. Zhang et al.<sup>[103]</sup> improved upon this approach by developing Ag/Sn–SnO<sub>2</sub> nanosheets which, through an adjusted electronic configuration, increased the active sites accessible for eCO<sub>2</sub>RR in comparison with Sn–SnO<sub>2</sub>, boosting the FE towards formate from 65% to 85% and halving H<sub>2</sub> formation from a FE of 40% to 20%.

Continuing the trend in catalyst innovation, Chen et al.<sup>[104]</sup> achieved a significant advance by engineering nano-crumpled within the Sn–Bi bimetallic interface. This design modification led to notable improvements in selectivity and stability for the eCO<sub>2</sub>RR to formate. By achieving an optimal upshift in the Sn p-band centre, this alteration weakens the Sn–C hybridization of the COOH\* intermediate and optimum Sn–O hybridization of HCOO\*. The comparison with pure Sn and Sn–Bi alloys revealed a marked increase in selectivity towards formate conversion. In-

depth in situ EXAFS and Raman spectroscopic analyses corroborated that the Sn–Bi bimetallic interface exhibits higher coordination numbers for Sn–Sn and Bi–Bi interactions, with a concurrent decrease for Sn–Bi pairings. This distinct coordination alters the bimetallic interface from the bulk alloy structure, facilitating prolonged electrode operation of 160 h, with a partial current density of  $40 \text{ mA cm}^{-2}$  and maintaining a FE of ca. 90% for formate production.

This line of investigation indicates that bimetallic systems are paving the way towards the development of more robust catalysts for  $\text{eCO}_2\text{RR}$ . The key to achieving long-term operational stability of such electrocatalysts lies in a profound understanding of the catalyst's mechanistic functions and the resultant impacts on the reaction pathway. The most extended operation duration reported, *i.e.* 2,400 h, was achieved using a  $\text{Bi}_{0.1}\text{Sn}$  catalyst as the cathode by Li et al.<sup>[105]</sup> This catalyst maintained a redox balance between Sn and  $\text{SnO}_2$  on the bimetallic active sites, which served to protect against corrosion and ensure longevity. With an FE exceeding 95% for over 170 h at  $100 \text{ mA cm}^{-2}$ , this  $\text{Bi}_{0.1}\text{Sn}$  catalyst demonstrated not only efficiency but also a promising route toward scaling up for pilot-scale  $\text{eCO}_2\text{RR}$  electrolyzers.

Such advancements herald a new era in catalyst design, one that could be instrumental in upscaling  $\text{eCO}_2\text{RR}$  processes to meet industrial demands. The detailed modifications and their effects outlined in the literature, summarized in Table S3, showcase the breadth of research dedicated to optimizing catalyst design for the electrochemical production of formate.

### 3.2.1.1. Metal-Free Catalysts for $\text{eCO}_2\text{RR}$ to Formate

In the quest for efficient  $\text{eCO}_2\text{RR}$  to formate, single-atom catalysts (SACs) have emerged as a bridge between homogeneous and heterogeneous catalysts, attracting significant attention in the last few years. These SACs capitalize on their unsaturated coordination sites and strong metal carrier interactions. This approach maximizes atomic utilization and ensures well-defined catalytic sites. Sun et al.<sup>[106]</sup> have extensively reviewed the challenges and opportunities associated with SACs in  $\text{eCO}_2\text{RR}$ , suggesting that these materials might significantly improve the  $\text{eCO}_2\text{RR}$  process through precise catalyst engineering.

### 3.2.2. Process Development/Reactor

Advancing  $\text{eCO}_2\text{RR}$  technology to an industrial scale requires a strategic approach to process development, including the design of reactors tailored for specific target products. The significance of process optimization at an industrial scale is increasingly highlighted in recent literature, reflecting a growing consensus on its critical role in the deployment of  $\text{eCO}_2\text{RR}$  technologies. Gao et al.<sup>[107]</sup> provide a comprehensive comparison of various electrolyzers used in  $\text{eCO}_2\text{RR}$ , ranging from H-cells to the impact of MEA cells on the process. The field has witnessed a notable shift from lower current densities to higher

ones ranging from  $50\text{--}1,000 \text{ mA cm}^{-2}$ , signifying a crucial development in reactor components specifically for  $\text{CO}_2$  electrolysis aimed at formate production. The significant advancements in reactor technology for the efficient conversion of  $\text{CO}_2$  to formate are outlined below:

#### 3.2.2.1. Modification of Electrolyzer: Three-Chamber Cell Design

Recent advancements in electrolyzer technology have focused on modifying the design of flow cells to directly produce concentrated FA, thereby reducing the costs associated with the downstream processing of converting formate to FA. For instance, solid-state electrolyzers have been tailored to yield high concentrations of FA. In a significant development, Yang et al.<sup>[108]</sup> introduced a novel three-chamber electrolyzer (figure 6) which uses a Sn GDE cathode embedded with imidazole ionomer. This design enhanced the  $\text{CO}_2$  concentration at the three-phase interface of the electrode and electrolyte, thereby improving the catalyst's selectivity for  $\text{eCO}_2\text{RR}$ . The modified cell demonstrated long-term stability, operating successfully for over 500 h with a current density of  $140 \text{ mA cm}^{-2}$  at a cell voltage of 3.5 V. Following a similar modification, Yang and co-workers were able to extend the operation time for 1,000 h using bismuth oxide ( $\text{Bi}_2\text{O}_3$ ) as the catalyst.<sup>[109]</sup> These three chamber electrolyzers feature an additional chamber that separates the catholyte and anolyte chambers using an AEM and CEM membrane, respectively. Deionized water flows through the middle chamber, allowing formate ions formed in the catholyte to migrate through the AEM and get protonated by protons from the anolyte passing through the CEM, thus forming FA. This design avoids the need for costly acidification processes typically required to separate formate salts.

Despite the improvements, the operational voltage of these systems, often above 4 V, remains higher than desirable for industrial applications. Furthermore, the initial catalyst stability lasted for 220 h before a decline in FA selectivity was observed.

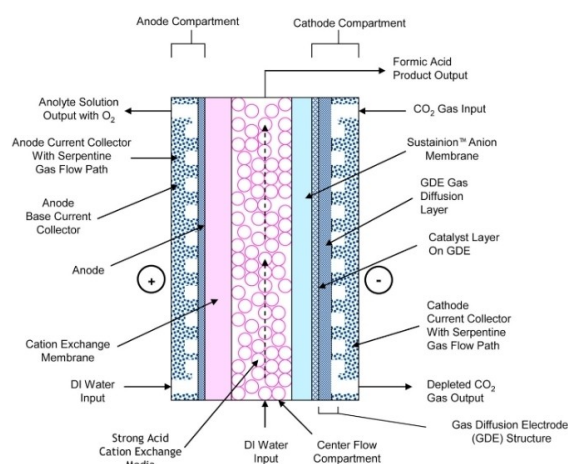


Figure 6. Formic acid 3-compartment cell configuration. Reproduced with permission<sup>[108]</sup> Copyright 2020, Elsevier.

To address this and ensure long-term stability, Einaga et al. applied a technique of reversing the polarization for a few seconds. This approach, known for modifying the surface termination in boron-doped diamond (BDD) electrodes,<sup>[110]</sup> effectively mitigates CO poisoning issues.<sup>[111]</sup> By periodically switching the polarization, the team achieved a continuous 1,000-hour operation with a reduced cell voltage ( $\leq 4$  V).

Although the three-chamber electrolyzer design has shown promising impacts on eCO<sub>2</sub>RR, the high cell voltage remains a significant challenge. This aspect holds potential for further improvement to meet industrial viability standards.

### 3.2.2.2. Membrane Modification

The membrane is a critical component in the design of electrolyzers, with its configuration playing a pivotal role in achieving industrially relevant operational cell potentials. A recent advancement in this area includes the use of a perforated CEM alongside an AEM within a zero-gap cell architecture. This innovative approach mimics the behavior of a BMP membrane while minimizing the impact on overall cell potential. In this setup, Bi<sub>2</sub>O<sub>3</sub> serves as the cathode material, and Pt/C is used as the anode. This modified membrane configuration has demonstrated impressive performance, achieving over 75% FE for FA production at cell potentials below 2 V and current densities of 300 mAcm<sup>-2</sup> in a 25 cm<sup>2</sup> cell.<sup>[112]</sup> Furthermore, during a stability test lasting 55 hours at 200 mAcm<sup>-2</sup>, both the FE and the cell voltage remained stable, underscoring the potential for long-term operation. A techno-economic analysis accompanying these experiments illustrates a viable pathway towards achieving cost parity with existing FA production methods,<sup>[112]</sup> suggesting significant potential for commercial application.

This development provides a promising direction for further exploration within the field of electrolyzer technology, particularly in terms of reducing cell potential and enhancing the overall energy efficiency of the system.

### 3.2.2.3. Solid-State Electrolyzers

Solid-state electrolyzers have been increasingly studied and optimized for eCO<sub>2</sub>RR,<sup>[81,107,113]</sup> offering promising solutions to the challenges associated with downstream processing. By eliminating the need for the separation of liquid products like FA and acetic acid from the electrolyte, solid electrolytes can significantly enhance cost-effectiveness.<sup>[114]</sup>

Xia et al.<sup>[115]</sup> demonstrated the production of high concentration (12 M) FA using a Bi electrode as the cathode within a solid electrolyte system. This system operated with a high selectivity toward formate (FE > 90%) for 100 h. The same group achieved even higher selectivity (FE  $\approx$  97%) and a partial current density of 450 mAcm<sup>-2</sup>. The authors also developed a solid-state eCO<sub>2</sub>RR system that continuously generates high-purity and high-concentration FA vapors and solutions. The system uses a porous solid electrolyte (PSE) layer to recombine

electrochemically generated formate and protons into molecular FA, which is then efficiently removed as vapors through an inert gas stream flowing through the PSE layer.<sup>[116]</sup> This approach achieved ultra-high concentrations of nearly 100 wt.% FA solutions, demonstrating the flexibility of tuning carrier gas streams.<sup>[116]</sup>

Further modifications were explored by Zhang et al.,<sup>[103]</sup> who combined the MEA with the PSE reactor, achieving stable operation for 200 h and producing 0.12 M FA using Ag/Sn-SnO<sub>2</sub> nanosheets as the catalyst. This catalyst was previously discussed in section 3.2.1 on catalyst design.

Additional advancements include modifications by Wang and co-workers, who utilized styrene-divinylbenzene copolymers as the base material for media development in solid-state electrolyzers.<sup>[115]</sup> Using Bi and Pt/C catalysts at the cathode and anode, respectively, they facilitated the recombination of formate and protons produced via eCO<sub>2</sub>RR and OER into FA. This FA was then efficiently removed by flowing deionized water through the PSE, achieving up to 0.1 M concentrations.

The quest towards making eCO<sub>2</sub>RR to FA/formate economically viable and sustainable for industry adoption has progressed significantly. With continuous improvements in engineering electrolyzers and electrode design through both multiphysics modelling and chemical modifications, the scientific community is addressing critical challenges such as ohmic losses arising at high current densities ( $j \geq 200$  mAcm<sup>-2</sup>) and enhancing the understanding of thermodynamics in solid electrolytes.<sup>[117]</sup>

## 3.3. Ethylene

Ethylene is a colorless, flammable unsaturated hydrocarbon that possesses a sweet taste and odor. In nature, it occurs as a hormone in plants, where it inhibits growth and promotes leaf fall, and in fruits, where it facilitates ripening. Its primary applications are split into two categories: as a monomer to form longer carbon chains, and as a foundational molecule for various two-carbon compounds. About fifty percent of ethylene's annual usage is in polymerization to produce polyethylene, commonly used in packaging films, wire coatings, and squeeze bottles. Ethylene is also a precursor for producing ethanol (industrial alcohol), ethylene oxide (converted into ethylene glycol for antifreeze and polyester fibers/films), acetaldehyde (which leads to acetic acid), vinyl chloride (converted to polyvinyl chloride, and ethylbenzene (converted to styrene for plastics and synthetic rubber production).<sup>[118,119]</sup>

Ethylene is sourced naturally from natural gas and petroleum. In the petrochemical industry, steam cracking is a primary production method, involving heating hydrocarbons and steam to 750–950 °C, which breaks larger hydrocarbons into smaller ones and introduces unsaturation. Depending on the raw materials (ethane, naphtha, gasoil, condensates), this process also yields propylene, C<sub>4</sub> olefins, and aromatics. Alternative methods include oxidative coupling of methane, Fischer-Tropsch synthesis, methanol-to-olefins, and catalytic dehydrogenation. However, conventional ethylene production methods

release significant greenhouse gases, including CO<sub>2</sub>, highlighting the need for sustainable practices.<sup>[118,119]</sup>

eCO<sub>2</sub>RR to ethylene presents several advantages over conventional methods. Key benefits include enhanced carbon utilization and integration with renewable energy sources. Unlike conventional techniques such as steam cracking of hydrocarbons, electrochemical reduction operates under milder conditions, with lower temperatures and pressures. The simplicity and scalability of the electrochemical process are notable advantages. As renewable energy costs continue to decline, the economic feasibility of this method improves, potentially making ethylene production cost competitive. Additionally, the ethylene produced can be seamlessly integrated into existing petrochemical infrastructure for further processing, facilitating adoption without requiring extensive modifications. In summary, eCO<sub>2</sub>RR to ethylene offers significant environmental and operational advantages over conventional methods, including enhanced sustainability, milder operating conditions, process simplicity, and potential cost savings through renewable energy integration.

### 3.3.1. Catalyst Design

Cu-based materials have shown promising results in eCO<sub>2</sub>RR due to their moderate CO adsorption capacity and suitable binding energy for the \*CO intermediate, which facilitates C–C coupling – a crucial step for ethylene generation.<sup>[120]</sup> The development of superior catalysts is critical to suppress the competing HER and enhance activity, selectivity, and stability towards ethylene. Research has focused on various catalyst types, including metallic, non-metallic molecular-based catalysts, multi-metal alloys, MOFs, and covalent organic frameworks, aiming to optimize activity, selectivity, and stability.<sup>[121]</sup> Factors influencing the performance of Cu-based catalysts in the eCO<sub>2</sub>RR to ethylene (C<sub>2</sub>H<sub>4</sub>) include catalyst morphology, surface oxidation state, the presence of surface defects, and crystal phase. These factors critically affect the adsorption and stabilization of key intermediates, such as CO and CHO, which are essential for C–C coupling leading to ethylene formation. Additionally, the local reaction environment near the Cu electrode, including the concentration of CO<sub>2</sub> and HCO<sub>3</sub><sup>−</sup> ions, as well as the local pH, can modulate the selectivity towards ethylene by influencing the surface-bound intermediates and the protonation steps.<sup>[121–123]</sup>

Achieving high selectivity for ethylene over competing products involves tuning the microenvironment at the three-phase interface and other properties such as local pH, cation, and anion effects, applied potential, and surface adsorption characteristics. These physical and/or chemical factors can have a major impact on the binding of key reaction intermediates along the eCO<sub>2</sub>RR process, resulting in the alteration of the reaction pathways, and therefore catalytic activity/selectivity. Theoretical investigations have identified promising reaction pathways for ethylene production, but scaling these pathways experimentally to an industrial level remains challenging.<sup>[49,124]</sup> Yet, a deep understanding of the mechanistic pathways can

guide modifications in the catalyst structure and composition, leveraging effects such as tip effect, defect engineering, crystal plane catalysis, synergistic effects, and nanoconfinement. Additionally, the properties of electrolytes (e.g., pH, CO<sub>2</sub> solubility, conductivity) play significant roles in determining catalytic performance and selectivity due to their direct contact with the active sites.<sup>[123,124]</sup>

Currently, the primary objective of eCO<sub>2</sub>RR to ethylene is the study of reaction mechanisms to enhance performance, with catalyst design through engineering remaining a top priority. This section 3.3 discusses several cutting-edge approaches for eCO<sub>2</sub>RR that focus on modulating the electronic and geometric properties of electrocatalysts. Approaches which aim to achieve breakthroughs in the eCO<sub>2</sub>RR to ethylene and other C<sub>2</sub>+ products include different synthesis techniques, surface modifications, optimizations of metal ratios, and the incorporation of molecular entities or organic frameworks (Table S4).

#### 3.3.1.1. Molecular Engineering and Surface Modification for Enhanced Cu Catalysts

Hu et al. explored the influence of incorporating electron-withdrawing groups derived from aromatic heterocycles on CO<sub>2</sub> reduction pathways.<sup>[125]</sup> By incorporating thiadiazole and triazole derivatives onto the surface of a bimetallic Ag–Cu catalyst, they significantly enhanced the formation of C<sub>2</sub>+ compounds. These modified electrodes achieved an impressive FE for C<sub>2</sub>+ products, ca. 80 ± 1%, and maintained robust stability over 100 hours.<sup>[125]</sup> This approach exemplifies how molecular engineering can manipulate the oxidation state of Cu electrodes to improve their eCO<sub>2</sub>RR performance.

In another significant study, Li et al. demonstrated a method to boost the activity of Cu catalysts towards ethylene by tuning their activity and interaction with reaction intermediates.<sup>[126]</sup> This was achieved by tailoring active sites on Cu–SiO<sub>x</sub> surfaces. Employed in an MEA electrolyzer, this catalyst achieved over 60% FE in ethylene production, sustaining current densities up to 300 mA cm<sup>−2</sup>. The ethylene energy efficiency (EE) reached 18% in the whole cell, with continuous operation for 55 hours under varying CO<sub>2</sub> concentrations (ranging from 10% to 100%).<sup>[126]</sup> Spectroscopic and electrochemical analyses, supported by DFT calculations, revealed that adding silica (SiO<sub>x</sub>) reduced the energy required for crucial reaction steps. This was attributed to the creation of strong bonds between silica and the Cu–SiO<sub>x</sub> surface, specifically at stable step sites, lowering the energy required for key intermediates and thus facilitating more efficient ethylene production. This advancement highlights new avenues in catalyst design for converting CO<sub>2</sub> into valuable products using oxide modifications.

Wen et al. introduced a novel design strategy by pre-designing stable Cu@S motifs within the HKUST-1 precatalyst framework, leading to a regenerative Cu(S) matrix that shows exceptional selectivity for ethylene, achieving FEs as high as 57.2% at a current density of 400 mA cm<sup>−2</sup>.<sup>[127]</sup> This activity and selectivity are among the highest reported for Cu-based metal-

organic species and MOFs used as electrocatalysts for eCO<sub>2</sub>RR. Operando X-ray absorption fine structure (XAFS) analysis and detailed characterizations provided compelling evidence of the Cu@S motif's stability throughout the eCO<sub>2</sub>RR process. The stabilized motif promoted more active Cu<sup>δ+</sup> species, significantly boosting catalytic activity. Theoretical studies underscored the critical role of S-stabilized Cu<sup>δ+</sup> species at the Cu/Cu<sub>x</sub>S<sub>y</sub> interface, optimizing geometric and electronic effects crucial for the \*CO dimerization process.

Xinyi Chen et al. explored a unique approach by decorating Cu electrodes with a stable amine-containing polymer exhibiting varying methylation degrees, hypothesizing that the polymer contributes to stabilizing intermediates during eCO<sub>2</sub>RR.<sup>[128]</sup> They developed a Cu-polyamine catalyst using a co-electroplating technique, which showed exceptionally high FE and EE for C<sub>2</sub> products. In a 1 M KOH electrolyte, the FE for ethylene production reached 72% (90% FE for C<sub>2</sub> products) at a cathode potential of  $-0.97 V_{\text{RHE}}$ . When the electrolyte concentration was increased to 10 M KOH, the FE for ethylene increased to 87% at  $-0.47 V_{\text{RHE}}$  (93% FE for C<sub>2</sub> products), with a full-cell EE of 50% at a cell potential of 2.02 V. In situ Raman spectroscopy revealed a higher surface pH, increased CO content, and more stabilized intermediates on the Cu-polyamine electrode compared to bare Cu or Cu with non-amine polymer additives during eCO<sub>2</sub>RR, indicating that intermediate stabilization and a higher surface pH can significantly enhance selectivity towards ethylene production.

Xie et al.<sup>[129]</sup> reported an innovative method by integrating gold nanoneedles into a copper porphyrin-based MOF, using carboxylates from the ligand as reducing agents for Au<sup>3+</sup> ions. This integration process led to the cleavage of connections between the ligand and the framework nodes, although it compromised the coherent structure of the framework. Remarkably, the inclusion of gold significantly enhanced the selectivity for ethylene production, achieving a FE of 52.5%, one of the highest reported for MOFs in existing literature. Extensive analysis using X-ray and infrared spectroscopies, along with DFT simulations, revealed that the increased ethylene selectivity was due to the presence of activated nitrogen motifs influenced by gold. These motifs worked in coordination with the copper centres within the metalloporphyrin, facilitating the coupling of C atoms at specific active sites. Additionally, the gold-enhanced catalyst showed improved stability in both structural integrity and catalytic performance. This improvement is likely attributed to a modified pathway for electrical conduction that helped to circumvent inconsistencies in the framework structure. This study underscores the potential of modifying the structure of metalloporphyrin networks through metal impregnation, directing the CO<sub>2</sub> reduction pathway and enhancing selectivity and stability.

In a notable study by Zu et al.,<sup>[130]</sup> copper hollow fiber penetration electrodes (Cu HPE) were employed for the eCO<sub>2</sub>RR to C<sub>2+</sub> products across a current density range of 0.1–3.0 A cm<sup>-2</sup> under highly acidic conditions (pH < 1). This study demonstrated that the elevated local proton consumption rate at higher current densities surpasses the bulk proton mass transport rate, thereby creating of a localized alkaline environment near the electrode.

This condition enhances the kinetics of the eCO<sub>2</sub>RR while effectively suppressing the competing HER.

Operating in a solution with a pH of 0.71, composed of H<sub>2</sub>SO<sub>4</sub> and KCl, the Cu HPE achieved remarkable selectivity, efficiency, and stability. Specific achievements included a high FE of 73.4%, a substantial partial current density of 2.2 A cm<sup>-2</sup>, and a notable single-pass carbon efficiency of 51.8% for C<sub>2+</sub> production, sustained over 100 hours of continuous operation. These performance metrics compare favorably with or even surpass those of state-of-the-art Cu-based catalysts.

The hollow-fiber configuration of the electrode ensures sufficient and continuous CO<sub>2</sub> delivery, which enhances CO<sub>2</sub> coverage on Cu active sites within the acidic environment. The co-adsorption of H<sup>+</sup> and K<sup>+</sup> ions on the electrode surface kinetically facilitates the protonation of \*CO and thermodynamically favors C–C coupling reactions. This process promotes both the activation of CO<sub>2</sub> and the formation of crucial intermediates, such as \*CHO and \*CO, thereby enhancing the subsequent C–C coupling reactions for the generation of C<sub>2+</sub> products.<sup>[130]</sup>

This innovative electrode structure engineering strategy presents a new avenue for achieving efficient and stable eCO<sub>2</sub>RR with high CO<sub>2</sub> utilization in acidic media, pointing towards the development of industrially feasible CO<sub>2</sub> electrolysis technologies.

In a separate investigation by Zhang et al.,<sup>[131]</sup> a versatile and scalable deposition-etch bombardment technique was developed to enhance the exposure of Cu(100) facets within nanostructured Cu films. This Cu(100)-enriched film showed superior performance as an electrode for catalyzing CO<sub>2</sub> reduction towards ethylene and C<sub>2+</sub> products. Within a flow cell setup, remarkable FEs of 58.6% for ethylene and 86.6% for C<sub>2+</sub> (including ethylene) were achieved. The deposition-etch bombardment method also streamlined the electrode assembly process, eliminating the need for polymer binders and improving the interface between the catalytic film and the substrate.

### 3.3.1.2. Oxide-Derived Cu Catalysts with Stable Interfaces

Liu et al., introduced an innovative anodic oxidation technique for large-scale production of oxide-derived Cu catalysts, featuring stable Cu/Cu<sub>2</sub>O interfaces crucial for active eCO<sub>2</sub>RR to ethylene.<sup>[132]</sup> By oxidizing Cu foil to form vertically aligned Cu nanoplates, the process maintained stable Cu/Cu<sub>2</sub>O interfaces during eCO<sub>2</sub>RR, preventing nanostructure clustering. The densely packed vertical lamellated-Cu (DVL–Cu) catalyst achieved an impressive FE and EE of 84.5% and 28.9% for ethylene, respectively, within a flow cell setup. In an MEA electrolyzer, it demonstrated an EE for ethylene of 27.6% at a current density of 200 mA cm<sup>-2</sup>, maintaining consistent performance for ca. 55 hours. Mechanistic analysis revealed that moderate current densities, uniform electrolyte current distribution, and elevated local pH collectively ensure structural and interfacial stability. Additionally, Cl<sup>-</sup> specific adsorption curtailed hydrogen evolution at higher overpotentials. Computational DFT studies highlighted the role of Cu<sup>+</sup> species in enhancing the adsorption capacity of the \*OCCOH intermediate, significantly reducing the energy barrier for C–C coupling.

Agapie and colleagues used a straightforward technique to structure copper electrodes at the nanoscale, utilizing  $N,N'$ -ethylene-phenanthroline dibromide as a molecular additive.<sup>[133]</sup> This approach achieved selectivities of up to 70% for  $C_2$  products over 40 hours, without significant alterations in surface morphology.<sup>[133]</sup> Mechanistic studies revealed that the organic additive induced cube-shaped nanostructure formation, stabilized these nanostructures during electrocatalysis through a protective organic layer, and promoted  $C_2$  product formation.

Luo et al. developed a method to adjust the morphologies of nano- $Cu_2O$  with various exposed facets, influencing morphology-dependent selectivity in  $eCO_2RR$ .<sup>[134]</sup> The highest FE for ethylene at 74.1% was achieved using step-structured  $Cu_2O$  nanoparticles with exposed (332) facets in a neutral electrolyte. DFT calculations revealed that these facets significantly reduce the free energy during the coupling of the  $*CHO$  intermediate, promoting ethylene production. This strategy offers a systematic approach to control product selectivity, enhancing the efficiency of  $CO_2$  recycling and green production of valuable carbon resources.<sup>[134]</sup>

### 3.3.1.3. Innovative Synthesis Methods for Enhanced Stability and Efficiency

In a study conducted by Wang and co-workers,<sup>[135]</sup> crystalline single-chain models, named as Cu-PzH, Cu-PzCl, Cu-PzBr, and Cu-PzI (Pz = pyrazole), were synthesized to investigate the selectivity of  $eCO_2RR$  products within a flow cell. The manipulation of the coordination microenvironment directly affected the selectivity between methane and ethylene. Notably, Cu-PzH demonstrated the highest FE for ethylene at 60%, with a substantial current density of  $346.46 \text{ mA cm}^{-2}$ . In contrast, as the substituent of the 4-XPz ligand transitioned from Cl to Br and then to I, the FE for ethylene decreased, while the FE for methane increased, with Cu-PzI showing the highest FE for methane at 52% and a current density of  $287.52 \text{ mA cm}^{-2}$ . Experimental observations and DFT calculations identified two key factors affecting these selectivity differences: the synergistic effect occurring between adjacent catalytically active sites, induced by variations in the coordination microenvironment, which influenced C–C coupling.

In research by Zhang et al.,<sup>[136]</sup> three  $Cu_1P_{13}$  catalysts with distinct morphologies –floculent, mixed, and spherical ( $Cu_1P_{13-0}$ ,  $Cu_1P_{13-6}$ ,  $Cu_1P_{13-24}$ )– were prepared by controlling the aging time. The  $eCO_2RR$  performance of these catalysts towards ethylene was evaluated in a flow cell, using an applied voltage of  $-1.4 V_{RHE}$  and 1 M KOH electrolyte. All three catalysts exhibited high current densities, with the spherical  $Cu_1P_{13-24}$  achieving the highest FE of 47% at a current density of  $350 \text{ mA cm}^{-2}$ . Characterization results indicated that electron interactions between Cu and P could be altered by modulating the morphology of copper phosphate. Notably, the spherical  $Cu_1P_{13-24}$  catalyst, compared to the other forms, promoted the formation of more  $Cu^+$  species favorable for the dimerization of  $*CO$  intermediates for C–C coupling to produce ethylene. Additionally, this catalyst demonstrated superior adsorption capacity for the key intermediate  $*CO$  and exhibited enhanced  $eCO_2RR$  performance. Stability tests showed that the  $Cu_1P_{13-24}$  catalyst maintained excellent current density and

ethylene selectivity for over 10 h, suggesting new avenues for improving the current density and selectivity of Cu/P catalysts by regulating morphology, providing a novel catalyst design strategy for efficient  $eCO_2RR$  to ethylene.

### 3.3.1.4. Innovative Cu-Based Tandem Catalysts and Cell Designs

Akter et al.<sup>[137]</sup> introduced tandem catalysts constructed on Ag electrodes, incorporating membrane-bound  $CuO_x$  nanoparticles, specifically designed for the selective  $eCO_2RR$  to ethylene. By altering the physical and chemical properties of the electrode architecture, they demonstrated that these catalysts operate via a stepwise pathway. Initially,  $CO_2$  is reduced to CO on the Ag surface, followed by further reduction to ethylene on the  $CuO_x$  nanoparticles. This method achieved FEs for ethylene production as high as 80%. Remarkably, an analogous Ag–Cu catalyst without the Nafion overlayer failed to produce any ethylene, emphasizing the crucial role of the polymer layer in regulating mass transport of the reactive CO intermediate and facilitating ethylene generation.

She et al.<sup>[138]</sup> demonstrated that a pure- $H_2O$ -fed alkali-cation-free APMA-MEA system effectively suppresses carbonate formation/precipitation and anion crossover during  $eCO_2RR$ , while also mitigating HER and losses of  $CO_2$  and electrolyte. This simple system design maintains an alkaline cathode environment without the need for alkali cations, enhancing system performance for  $eCO_2RR$ . Their experiments also showed that the APMA system could operate continuously for over 1,000 h without  $CO_2$  or electrolyte losses in six-APMA-MEA cell stack, achieving an ethylene-specific FE of 50% at 10 A ( $300 \text{ mA cm}^{-2}$  for single MEA cell). Although the system displayed competitive performance for ethylene production, further improvements in product selectivity and operation voltage reduction are needed for more efficient energy conversion.

Moller et al.<sup>[139]</sup> designed and analyzed the first full low-temperature tandem electrolyzer cell system aimed at efficient  $eCO_2RR$  to  $C_{2+}$  products, such as ethylene, ethanol, and propanol. This tandem design involved two low-temperature electrolyzer cells in series, enabling a catalytic reaction cascade from  $CO_2$  to mix  $CO_2/CO$  streams in the first cell, then converting the mixed  $CO_2/CO$  feeds to  $C_{2+}$  products in the second cell. They utilized a noble metal-free single Ni atom site electrocatalyst (Ni–N–C) in the first cell and a Cu-catalyst in the second. This setup strongly enhanced the production rates of ethylene (*ca.* 50%) and alcohols with a significantly increased  $C_{2+}$  energy efficiency compared to conventional single  $CO_2$  electrolyzer approaches. Control experiments with mixed  $CO_2/CO$  co-feeds provided insights into the tandem effect, suggesting selective scrubbing of  $CO_2$  by cathodically generated  $OH^-$ , thus locally increasing the effective CO concentration and surface coverage, mimicking the performance of CO-rich gas feeds. The tandem system also demonstrated enhanced production rates of  $C_{2+}$  compounds and was more energy-efficient compared to the conventional single-cell system, underscoring the potential of this innovative approach.

In recent studies by Zhang et al.,<sup>[140]</sup> the combination of computation analysis and experimental results is used to determine the rate-limiting step to resolve the complex mechanistic pathways involved in ethylene production. This approach can prove to be effective to enhance the faradaic efficiency, selectivity and energy efficiency of the system. They reveal that C–C bond-making is the RDS on Cu(100), whereas the protonation of \*CO with adsorbed water becomes rate-limiting on Cu(111) with a higher energy barrier. On an oxide-derived Cu(100)-dominant Cu catalyst, they achieved a high C<sub>2</sub>H<sub>4</sub> Faradaic efficiency of 72%, partial current density of 359 mAcm<sup>-2</sup>, and long-term stability exceeding 100 h at 500 mAcm<sup>-2</sup>, greatly outperforming its Cu(111)-rich counterpart. Further demonstration with MEA electrolyzer had constant C<sub>2</sub>H<sub>4</sub> selectivity of >60% over 70 h with a full-cell energy efficiency of 23.4%.

### 3.3.2. Reactor

Flow cell reactors are often used in research and pilot-scale applications due to uncomplicated design for ethylene production from eCO<sub>2</sub>RR. In these reactors, various catalyst materials (such as copper-based catalysts<sup>[140]</sup>) and electrolyte compositions are used to optimize the electrochemical conversion of CO<sub>2</sub> to ethylene. The choice of reactor type depends on the specific application, scale, and desired outcomes of the eCO<sub>2</sub>RR process.

## 4. Current Challenges Toward eCO<sub>2</sub>RR Commercialization

We had discussed before in section 2.1 about different products and complexities toward commercialization of eCO<sub>2</sub>RR technology. Several critical challenges, regardless of the product, must be addressed to scale up eCO<sub>2</sub>RR technology for commercialization, despite its promise for sustainable manufacturing. These challenges include:

1. Low carbon conversion efficiencies<sup>[141]</sup>
2. Competing HER reaction
3. Poor electrocatalyst stability and selectivity
4. Mass transfer limitation for multicarbon products
5. High energy consumption
6. Lack of suitable, efficient, scalable components and reactor design
7. Operational issues like salt precipitation, flooding, electrode degradation.<sup>[142]</sup>

Research and development efforts continue to focus on addressing these challenges, aiming to make the electrochemical conversion as competitive as traditional methods. There has always been a trade-off or tug-of-war-like situation among multiple parameters for the advancement of the eCO<sub>2</sub>RR technologies. But currently looking at the scientific progress it is always about choosing one parameter over another and compromising the least valued parameter. Currently, viable solutions for above mentioned challenges and operational issues include a combination of different ion exchange membranes with suitable electrolytes,

designing advanced catalysts, electrolyte recirculation for removing salt, recirculation of CO<sub>2</sub> obtained from salts. We believe better understanding of the reaction mechanism and iterative fundamental research toward electrocatalyst, reactor design for electrolyte management will lead to most promising technology in future.

## 5. Summary and Outlook

In summary, this review highlights gaps between lab-based and industrial-scale electrochemical CO<sub>2</sub> reduction (eCO<sub>2</sub>RR). We found a significant lack of collaboration in areas such as basic electrochemical analysis, catalyst development, statistical methods, engineering, and economic feasibility. These gaps hinder the industrial development and commercialization of eCO<sub>2</sub>RR technology. We argue that the progress of eCO<sub>2</sub>RR technology depends on creating an environment that supports these crucial components.

We examined the economic implications and industrial outlook of eCO<sub>2</sub>RR products, presenting minimum criteria for industrial deployment and conducting comparative analyses among various products. These analyses underscore the substantial opportunities within the eCO<sub>2</sub>RR domain, especially given the current market landscape. Furthermore, we elaborated on the technological aspects and recent research findings concerning three pivotal eCO<sub>2</sub>RR products: carbon monoxide, formic acid, and ethylene. The discussion encompassed reactor configurations and operational parameters, recognizing the potentially transformative impact of these products on the future trajectory of eCO<sub>2</sub>RR technology in alignment with sustainability objectives. While innovative catalyst design strategies and reactor modifications have demonstrated enhanced performance in eCO<sub>2</sub>RR, challenges persist in the commercialization pathway, particularly concerning C<sub>2/2+</sub> products. Nevertheless, C<sub>1</sub> products present promising avenues for advancing towards market integration.

## Acknowledgements

The authors A.G., G.C., M.G.-M. and D.P. acknowledge the support from the European Union's Horizon 2021 programme under the Marie Skłodowska-Curie Doctoral Networks (MSCA-DN) grant agreement No 101072830 (ECOMATES). S.V. and J.H. acknowledge the support from the European Union's Horizon 2020 research and innovation programme under grant agreement no. 101037389 (ECO<sub>2</sub>FUEL). Additionally, D.P. acknowledge the support from the European Union's Horizon 2020 project VIVALDI (grant agreement no. 101000441), the European Union's Horizon Europe project FUELS-C (grant agreement No 101147442) and Flanders Innovation & Entrepreneurship (VLAIO) under project no. HBC.2021.0586 (CLUE).

## Conflict of Interests

There are no conflicts to declare.

## Data Availability Statement

Data sharing is not applicable to this article as no new data were created or analyzed in this study.

**Keywords:** Industrial eCO<sub>2</sub>RR · Sustainability · Techno-economic · Ecosystem · Catalyst design

- [1] L. J. R. Nunes, *Environ.* **2023**, *10*, 66.
- [2] D. Xu, K. Li, B. Jia, W. Sun, W. Zhang, X. Liu, T. Ma, *Carbon Energy* **2023**, *5*, e230.
- [3] C. Ren, W. Ni, H. Li, *Catalysts* **2023**, *13*, 644.
- [4] K. M. Diederichsen, R. Sharifian, J. S. Kang, Y. Liu, S. Kim, B. M. Gallant, D. Vermaas, T. A. Hatton, *Nat. Rev. Methods Primers* **2022**, *2*, 68.
- [5] O. S. Bushuyev, P. de Luna, C. T. Dinh, L. Tao, G. Saur, J. van de Lagemaat, S. O. Kelley, E. H. Sargent, *Joule* **2018**, *2*, 825.
- [6] O. G. Sánchez, Y. Y. Birdja, M. Bulut, J. Vaes, T. Breugelmans, D. Pant, *Curr. Opin. Green Sustain. Chem.* **2019**, *16*, 47.
- [7] J. Song, Y. Y. Birdja, D. Pant, Z. Chen, J. Vaes, *Int. J. Miner. Metall. Mater.* **2022**, *29*, 848.
- [8] K. C. Poon, W. Y. Wan, H. Su, H. Sato, *RSC Adv.* **2022**, *12*, 22703.
- [9] D. Wakerley, S. Lamaison, J. Wicks, A. Clemens, J. Feaster, D. Corral, S. A. Jaffer, A. Sarkar, M. Fontecave, E. B. Duoss et al., *Nat Energy* **2022**, *7*, 130.
- [10] I. E. L. Stephens, K. Chan, A. Bagger, S. W. Boettcher, J. Bonin, E. Boutin, A. K. Buckley, R. Buonsanti, E. R. Cave, X. Chang et al., *J. Phys. Energy* **2022**, *4*, 42003.
- [11] Z. Gu, H. Shen, Z. Chen, Y. Yang, C. Yang, Y. Ji, Y. Wang, C. Zhu, J. Liu, J. Li et al., *Joule* **2021**, *5*, 429.
- [12] J. M. Álvarez-Gómez, A. S. Varela, *Energy Fuels* **2023**, *37*, 15283.
- [13] S. Varhade, E. B. Tetteh, S. Saddeler, S. Schumacher, H. B. Aiyappa, G. Bendt, S. Schulz, C. Andronescu, W. Schuhmann, *Chemistry (Weinheim an der Bergstrasse, Germany)* **2023**, *29*, e202203474.
- [14] E. B. Tetteh, L. Banko, O. A. Krysiak, T. Löffler, B. Xiao, S. Varhade, S. Schumacher, A. Sazan, C. Andronescu, A. Ludwig et al., *Electrochem. Sci. Adv.* **2022**, *2*, e2100105.
- [15] S. Schumacher, L. Madau, Y. Liebsch, E. B. Tetteh, S. Varhade, W. Schuhmann, M. Schleberger, C. Andronescu, *ChemElectroChem* **2022**, *9*, e202200586.
- [16] S. S. A. Shah, M. Sufyan Javed, T. Najam, C. Molochas, N. A. Khan, M. A. Nazir, M. Xu, P. Tsiakaras, S.-J. Bao, *Coord. Chem. Rev.* **2022**, *471*, 214716.
- [17] D. Segets, C. Andronescu, U.-P. Apfel, *Nat. Commun.* **2023**, *14*, 7950.
- [18] H. Shin, K. U. Hansen, F. Jiao, *Nat. Sustain.* **2021**, *4*, 911.
- [19] H. Kildahl, L. Wang, L. Tong, H. Cao, Y. Ding, *J. CO<sub>2</sub> Util.* **2022**, *65*, 102181.
- [20] C. Hepburn, E. Adlen, J. Beddington, E. A. Carter, S. Fuss, N. Mac Dowell, J. C. Minx, P. Smith, C. K. Williams, *Nature* **2019**, *575*, 87.
- [21] X. Zhang, W. Huang, L. Yu, M. García-Melchor, D. Wang, L. Zhi, H. Zhang, *Carbon Energy* **2024**, *6*, e362.
- [22] M. H. Barecka, J. W. Ager, A. A. Lapkin, *STAR Protoc.* **2021**, *2*, 100889.
- [23] T. Alerte, A. Gaona, J. P. Edwards, C. M. Gabardo, C. P. O'Brien, J. Wicks, L. Bonnenfant, A. S. Rasouli, D. Young, J. Abed et al., *ACS Sustain. Chem. Eng.* **2023**, *11*, 15651.
- [24] J. W. Blake, V. Konderla, L. M. Baumgartner, D. A. Vermaas, J. T. Padding, J. W. Haverkort, *ACS Sustain. Chem. Eng.* **2023**, *11*, 2840.
- [25] B. Pribyl-Kranewitter, A. Beard, C. L. Gijiu, D. Dinculescu, T. J. Schmidt, *Renew. Sustain. Energy Rev.* **2022**, *154*, 111807.
- [26] X. Zhang, S.-X. Guo, K. A. Gandionco, A. M. Bond, J. Zhang, *Mater. Today Adv.* **2020**, *7*, 100074.
- [27] R. C. Fortenberry, C. M. Novak, T. J. Lee, P. P. Bera, J. E. Rice, *ACS Omega* **2018**, *3*, 16035.
- [28] N. T. Thuy Tran, S.-Y. Lin, O. E. Glukhova, M.-F. Lin, *RSC Adv.* **2016**, *6*, 24458.
- [29] Y. Y. Birdja, E. Pérez-Gallent, M. C. Figueiredo, A. J. Göttle, F. Calle-Vallejo, M. T. M. Koper, *Nat. Energy* **2019**, *4*, 732.
- [30] Y. Y. Birdja, J. Vaes, *ChemElectroChem* **2020**, *7*, 4713.
- [31] Y. Zou, S. Wang, *Adv. Sci.* **2021**, *8*, 2003579.
- [32] J. Durst, A. Rudnev, A. Dutta, Y. Fu, J. Herranz, V. Kaliginedi, A. Kuzume, A. A. Permyakova, Y. Paratcha, P. Broekmann et al., *Chimia* **2015**, *69*, 769.
- [33] Z. Sun, T. Ma, H. Tao, Q. Fan, B. Han, *Chem* **2017**, *3*, 560.
- [34] B. Belsa, L. Xia, V. Golovanova, B. Polesso, A. Pinilla-Sánchez, L. San Martín, J. Ye, C.-T. Dinh, F. P. García de Arquer, *Nat. Rev. Mater.* **2024**, *9*, 535.
- [35] L. Fan, C. Xia, F. Yang, J. Wang, H. Wang, Y. Lu, *Sci. Adv.*, *6*, eaay3111.
- [36] Y. Meng, H. Huang, Y. Zhang, Y. Cao, H. Lu, X. Li, *Front. Chem.* **2023**, *11*, 1172146.
- [37] Z. Zhang, Y. Zheng, L. Qian, D. Luo, H. Dou, G. Wen, A. Yu, Z. Chen, *Adv. Mater.* **2022**, *34*, e2201547.
- [38] P. Wang, M. Qiao, Q. Shao, Y. Pi, X. Zhu, Y. Li, X. Huang, *Nat. Commun.* **2018**, *9*, 4933.
- [39] P. Sun, S. Liu, X. Zheng, G. Hu, Q. Zhang, X. Liu, G. Zheng, Y. Chen, *Nano Today* **2024**, *55*, 102152.
- [40] Q. Lu, F. Jiao, *Nano Energy* **2016**, *29*, 439.
- [41] G. Kastlunger, H. H. Heenen, N. Govindarajan, *ACS Catal.* **2023**, *13*, 5062.
- [42] K. Chan, *Nat. Commun.* **2020**, *11*, 5954.
- [43] A. Rendón-Calle, S. Builes, F. Calle-Vallejo, *Curr. Opin. Electrochem.* **2018**, *9*, 158.
- [44] F. Yu, K. Deng, M. Du, W. Wang, F. Liu, D. Liang, *Carbon Capture Sci. Technol.* **2023**, *6*, 100081.
- [45] D. Misra, G. Di Liberto, G. Pacchioni, *Phys. Chem. Chem. Phys.* **2024**, *26*, 10746.
- [46] M. Suvarna, J. Pérez-Ramírez, *Nat. Catal.* **2024**, *7*, 624.
- [47] M. Jun, J. Kundu, D. H. Kim, M. Kim, D. Kim, K. Lee, S.-I. Choi, *Adv. Mater.* **2024**, *36*, e2313028.
- [48] S. Nitopi, E. Bertheussen, S. B. Scott, X. Liu, A. K. Engstfeld, S. Horch, B. Seger, I. E. L. Stephens, K. Chan, C. Hahn et al., *Chem. Rev.* **2019**, *119*, 7610.
- [49] M. Jouny, W. Luc, F. Jiao, *Ind. Eng. Chem. Res.* **2018**, *57*, 2165.
- [50] J. P. Edwards, T. Alerte, C. P. O'Brien, C. M. Gabardo, S. Liu, J. Wicks, A. Gaona, J. Abed, Y. C. Xiao, D. Young et al., *ACS Energy Lett.* **2023**, *8*, 2576.
- [51] M. S. Sajna, S. Zavahir, A. Popelka, P. Kasak, A. Al-Sharshani, U. Onwusogh, M. Wang, H. Park, D. S. Han, *J. Environ. Chem. Eng.* **2023**, *11*, 110467.
- [52] J. Wu, T. Sharifi, Y. Gao, T. Zhang, P. M. Ajayan, *Adv. Mater.* **2019**, *31*, e1804257.
- [53] M. G. Kibria, J. P. Edwards, C. M. Gabardo, C.-T. Dinh, A. Seifitokaldani, D. Sinton, E. H. Sargent, *Adv. Mater.* **2019**, *31*, 1807166.
- [54] R. A. Tufa, D. Chanda, M. Ma, D. Aili, T. B. Demissie, J. Vaes, Q. Li, S. Liu, D. Pant, *Appl. Energy* **2020**, *277*, 115557.
- [55] M. König, S.-H. Lin, J. Vaes, D. Pant, E. Klemm, *Faraday Discuss.* **2021**, *230*, 360.
- [56] J. van de Loosdrecht, J. W. Niemantsverdriet (Ed: R. Schlögl), *De Gruyter*, **2013**, 443–458.
- [57] M. E. Dry, *Catal. Today* **2002**, *71*, 227.
- [58] R. Schlögl (Ed.), *De Gruyter*, **2013**.
- [59] P. Debergh, O. Gutiérrez-Sánchez, M. N. Khan, Y. Y. Birdja, D. Pant, M. Bulut, *ACS Energy Lett.* **2023**, *8*, 3398.
- [60] C. Mittal, C. Hadsbjerg, P. Blennow, *Chem. Eng. World* **2017**, *52*, 44.
- [61] S. Verma, Y. Hamasaki, C. Kim, W. Huang, S. Lu, H.-R. M. Jhong, A. A. Gewirth, T. Fujigaya, N. Nakashima, P. J. A. Kenis, *ACS Energy Lett.* **2018**, *3*, 193.
- [62] Y. Hori, H. Konishi, T. Futamura, A. Murata, O. Koga, H. Sakurai, K. Oguma, *Electrochim. Acta* **2005**, *50*, 5354.
- [63] T. Zheng, K. Jiang, H. Wang, *Adv. Mat.* **2018**, *30*, e1802066.
- [64] E. Sedano Varo, R. Egeberg Tankard, J. Kryger-Baggesen, J. Jinschek, S. Helveg, I. Chorkendorff, C. D. Damsgaard, J. Kibsgaard, *JACS* **2024**, *146*, 2015.
- [65] J. Fu, W. Zhu, Y. Chen, Z. Yin, Y. Li, J. Liu, H. Zhang, J.-J. Zhu, S. Sun, *Angew. Chem. Int. Ed. Engl.* **2019**, *131*, 14238.
- [66] A. M. Ismail, E. Csapó, C. Janáky, *Electrochim. Acta* **2019**, *313*, 171.
- [67] W. Zhu, Y.-J. Zhang, H. Zhang, H. Lv, Q. Li, R. Michalsky, A. A. Peterson, S. Sun, *JACS* **2014**, *136*, 16132.
- [68] D. R. Kauffman, D. Alfonso, C. Matranga, H. Qian, R. Jin, *JACS* **2012**, *134*, 10237.
- [69] M. Liu, Y. Pang, B. Zhang, P. de Luna, O. Voznyy, J. Xu, X. Zheng, C. T. Dinh, F. Fan, C. Cao et al., *Nature* **2016**, *537*, 382.
- [70] J. Kim, J. T. Song, H. Ryoo, J.-G. Kim, S.-Y. Chung, J. Oh, *J. Mater. Chem. A* **2018**, *6*, 5119.
- [71] J. He, N. J. J. Johnson, A. Huang, C. P. Berlinguette, *ChemSusChem* **2018**, *11*, 48.
- [72] J. Lee, J. Lim, C.-W. Roh, H. S. Whang, H. Lee, *J. CO<sub>2</sub> Util.* **2019**, *31*, 244.
- [73] B. A. Rosen, A. Salehi-Khojin, M. R. Thorson, W. Zhu, D. T. Whipple, P. J. A. Kenis, R. I. Masel, *Science* **2011**, *334*, 643.

- [74] S. Chandrashekar, H. Geerlings, W. A. Smith, *ChemElectroChem* **2021**, *8*, 4515.
- [75] J. W. Park, W. Choi, J. Noh, W. Park, G. H. Gu, J. Park, Y. Jung, H. Song, *ACS Appl. Mater. Interfaces* **2022**, *14*, 6604.
- [76] H. Noda, S. Ikeda, Y. Oda, K. Imai, M. Maeda, K. Ito, *Bull. Chem. Soc. Jpn.* **1990**, *63*, 2459.
- [77] W. Luo, J. Zhang, M. Li, A. Züttel, *ACS Catal.* **2019**, *9*, 3783.
- [78] L. Wang, H. Peng, S. Lamaison, Z. Qi, D. M. Koshy, M. B. Stevens, D. Wakerley, J. A. Zamora Zeledón, L. A. King, L. Zhou et al., *Chem Catal.* **2021**, *1*, 663.
- [79] X. Li, X. Wu, X. Lv, J. Wang, H. B. Wu, *Chem. Catal.* **2022**, *2*, 262.
- [80] H. Xie, S. Chen, F. Ma, J. Liang, Z. Miao, T. Wang, H.-L. Wang, Y. Huang, Q. Li, *ACS Appl. Mater. Interfaces* **2018**, *10*, 36996.
- [81] F.-Y. Gao, R.-C. Bao, M.-R. Gao, S.-H. Yu, *J. Mater. Chem. A* **2020**, *8*, 15458.
- [82] I. M. Badawy, A. M. Ismail, G. E. Khedr, M. M. Taha, N. K. Allam, *Sci. Rep.* **2022**, *12*, 13456.
- [83] R. Küngas, *J. Electrochem. Soc.* **2020**, *167*, 44508.
- [84] M. Quentmeier, B. Schmid, H. Tempel, R.-A. Eichel, *ACS Sustain. Chem. Eng.* **2024**, *12*, 3876.
- [85] R. B. Kutz, Q. Chen, H. Yang, S. D. Sajjad, Z. Liu, I. R. Masel, *Energy Tech.* **2017**, *5*, 929.
- [86] D. A. Bulushev, J. R. H. Ross, *ChemSusChem* **2018**, *11*, 821.
- [87] A. Irabien, M. Alvarez-Guerra, J. Albo, A. Dominguez-Ramos in *Electrochemical Water and Wastewater Treatment* (Eds: C. A. Martinez-Huitile, M. A. Rodrigo, O. Scialdone), Butterworth-Heinemann, **2018**, 29–59.
- [88] S. Chatterjee, I. Dutta, Y. Lum, Z. Lai, K.-W. Huang, *Energy Environ. Sci.* **2021**, *14*, 1194.
- [89] X. Chen, Y. Liu, J. Wu, *Mol. Catal.* **2020**, *483*, 110716.
- [90] X. Christodoulou, T. Okoroafor, S. Parry, S. B. Velasquez-Orta, *J. CO<sub>2</sub> Util.* **2017**, *18*, 390.
- [91] Z. Masoumi, M. Tayebi, M. Tayebi, S. A. Masoumi Lari, N. Sewwandi, B. Seo, C.-S. Lim, H.-G. Kim, D. Kyung, *Int. J. Mol. Sci.* **2023**, *24*, 9952.
- [92] Y. Hori, *Modern Aspects of Electrochemistry* (Eds: C. G. Vayenas, R. E. White, M. E. Gamboa-Aldeco), Springer New York, New York, NY, **2008**, 89–189.
- [93] P. Duarah, D. Haldar, V. S. Yadav, M. K. Purkait, *J. Environ. Chem. Eng.* **2021**, *9*, 106394.
- [94] N. Han, P. Ding, L. He, Y. Li, Y. Li, *Adv. Energy Mater.* **2020**, *10*, 1902338.
- [95] J. Zou, G. Liang, C.-Y. Lee, G. G. Wallace, *Mater. Today Energy* **2023**, *38*, 101433.
- [96] K. van Daele, B. de Mot, M. Pupo, N. Daems, D. Pant, R. Kortlever, T. Breugelmans, *ACS Energy Lett.* **2021**, *6*, 4317.
- [97] T. Ouyang, S. Huang, X.-T. Wang, Z.-Q. Liu, *Chem. Eur. J.* **2020**, *26*, 14024.
- [98] G. Wang, X. Li, X. Yang, L.-X. Liu, Y. Cai, Y. Wu, S. Wang, H. Li, Y. Zhou, Y. Wang et al., *Chem. Eur. J.* **2022**, *28*, e202201834.
- [99] Y. Wang, J. Liu, Y. Wang, A. M. Al-Enizi, G. Zheng, *Small* **2017**, *13*, 1701809.
- [100] C. H. Lee, M. W. Kanan, *ACS Catal.* **2015**, *5*, 465.
- [101] S. Liang, J. Xiao, T. Zhang, Y. Zheng, Q. Wang, B. Liu, *Angew. Chem. Int. Ed.* **2023**, *62*, e202310740.
- [102] Z. Chen, D. Zhang, Q. Li, H. Zhang, Y. Zhao, Q. Ke, Y. Yan, L. Liu, M. Liu, X. He, *Appl. Catal. B* **2024**, *341*, 123342.
- [103] M. Zhang, A. Cao, Y. Xiang, C. Ban, G. Han, J. Ding, L.-Y. Gan, X. Zhou, *Nano-Micro Lett.* **2023**, *16*, 50.
- [104] B. Ren, G. Wen, R. Gao, D. Luo, Z. Zhang, W. Qiu, Q. Ma, X. Wang, Y. Cui, L. Ricardez-Sandoval et al., *Nat. Commun.* **2022**, *13*, 2486.
- [105] L. Li, A. Ozden, S. Guo, G. de Arquer, F. Pelayo, C. Wang, M. Zhang, J. Zhang, H. Jiang, W. Wang, H. Dong, et al., *Nat. Commun.* **2021**, *12*, 5223.
- [106] P. Sun, S. Liu, X. Zheng, G. Hu, Q. Zhang, X. Liu, G. Zheng, Y. Chen, *Nano Today* **2024**, *55*, 102152.
- [107] G. Gao, C. A. Obasanjo, J. Crane, C.-T. Dinh, *Catal. Today* **2023**, *423*, 114284.
- [108] H. Yang, J. J. Kaczur, S. D. Sajjad, R. I. Masel, *J. CO<sub>2</sub> Util.* **2017**, *20*, 208.
- [109] H. Yang, J. J. Kaczur, S. D. Sajjad, R. I. Masel, *J. CO<sub>2</sub> Util.* **2020**, *42*, 101349.
- [110] N. Ikemiya, K. Natsui, K. Nakata, Y. Einaga, *ACS Sustain. Chem. Eng.* **2018**, *6*, 8108.
- [111] C. W. Lee, N. H. Cho, K. T. Nam, Y. J. Hwang, B. K. Min, *Nat. Commun.* **2019**, *10*, 3919.
- [112] L. Hu, J. A. Wrubel, C. M. Baez-Cotto, F. Intia, J. H. Park, A. J. Kropf, N. Kariuki, Z. Huang, A. Farghaly, L. Amichi et al., *Nat. Commun.* **2023**, *14*, 7605.
- [113] Y. Kang, T. Kim, K. Y. Jung, K. T. Park, *Catalysts* **2023**, *13*, 955.
- [114] J. Li, Z. Wang, S. Liu, Z. Chen, J. Yang, Z. Chen, A. Li, Q. Wen, L. Wang, S. Qiu et al., *Chem. Eng. J.* **2024**, *481*, 148452.
- [115] C. Xia, P. Zhu, Q. Jiang, Y. Pan, W. Liang, E. Stavitski, H. N. Alshareef, H. Wang, *Nat. Energy* **2019**, *4*, 776.
- [116] L. Fan, C. Xia, P. Zhu, Y. Lu, H. Wang, *Nat. Commun.* **2020**, *11*, 3633.
- [117] W. Zhang, H. Shan, Y. Liu, Q. Xu, H. Su, Q. Ma, H. Liu, L. Hua, Z. Li, *Chem. Phys. Lett.* **2024**, *836*, 141031.
- [118] Y. Gao, L. Neal, D. Ding, W. Wu, C. Baroi, A. M. Gaffney, F. Li, *ACS Catal.* **2019**, *9*, 8592.
- [119] P. Lamichhane, N. Pourali, L. Scott, N. N. Tran, L. Lin, M. E. Gelonch, E. V. Rebrov, V. Hessel, *Renew. Sustain. Energy Rev.* **2024**, *189*, 114044.
- [120] W. Deng, P. Zhang, Y. Qiao, G. Kastlunger, N. Govindarajan, A. Xu, I. Chorkendorff, B. Seger, J. Gong, *Nat. Commun.* **2024**, *15*, 892.
- [121] F. Wang, Z. Lu, H. Guo, G. Hao, W. Jiang, G. Liu, *Coord. Chem. Rev.* **2024**, *515*, 215962.
- [122] Y. Mi, X. Peng, X. Liu, J. Luo, *ACS Appl. Energy Mater.* **2018**, *1*, 5119.
- [123] A. S. Varela, W. Ju, T. Reier, P. Strasser, *ACS Catal.* **2016**, *6*, 2136.
- [124] X. Liu, J. Xiao, H. Peng, X. Hong, K. Chan, J. K. Nørskov, *Nat. Commun.* **2017**, *8*, 15438.
- [125] H. Wu, J. Li, K. Qi, Y. Zhang, E. Petit, W. Wang, V. Flaud, N. Onofrio, B. Rebriere, L. Huang et al., *Nat. Commun.* **2021**, *12*, 7210.
- [126] J. Li, A. Ozden, M. Wan, Y. Hu, F. Li, Y. Wang, R. R. Zamani, D. Ren, Z. Wang, Y. Xu et al., *Nat. Commun.* **2021**, *12*, 2808.
- [127] C. F. Wen, M. Zhou, P. F. Liu, Y. Liu, X. Wu, F. Mao, S. Dai, B. Xu, X. L. Wang, Z. Jiang et al., *Angew. Chem. Int. Ed. Engl.* **2022**, *61*, e202111700.
- [128] X. Chen, J. Chen, N. M. Alghoraibi, D. A. Henckel, R. Zhang, U. O. Nwabara, K. E. Madsen, P. J. A. Kenis, S. C. Zimmerman, A. A. Gewirth, *Nat. Catal.* **2021**, *4*, 20.
- [129] X. Xie, X. Zhang, M. Xie, L. Xiong, H. Sun, Y. Lu, Q. Mu, M. H. Rummeli, J. Xu, S. Li et al., *Nat. Commun.* **2022**, *13*, 63.
- [130] C. Zhu, G. Wu, A. Chen, G. Feng, X. Dong, G. Li, S. Li, Y. Song, W. Wei, W. Chen, *Energy Environ. Sci.* **2024**, *17*, 510.
- [131] G. Zhang, Z.-J. Zhao, D. Cheng, H. Li, J. Yu, Q. Wang, H. Gao, J. Guo, H. Wang, G. A. Ozin et al., *Nat. Commun.* **2021**, *12*, 5745.
- [132] W. Liu, P. Zhai, A. Li, B. Wei, K. Si, Y. Wei, X. Wang, G. Zhu, Q. Chen, X. Gu et al., *Nat. Commun.* **2022**, *13*, 1877.
- [133] A. Thevenon, A. Rosas-Hernández, J. C. Peters, T. Agapie, *Angew. Chem. Int. Ed.* **2019**, *58*, 16952.
- [134] H. Luo, B. Li, J.-G. Ma, P. Cheng, *Angew. Chem. Int. Ed.* **2022**, *61*, e202116736.
- [135] R. Wang, J. Liu, Q. Huang, L.-Z. Dong, S.-L. Li, Y.-Q. Lan, *Angew. Chem. Int. Ed. Engl.* **2021**, *60*, 19829.
- [136] L. Zhang, Y. Men, B. Wu, Y. Feng, C. Song, S. Liu, J. Wang, W. An, T. T. Magkoev, *Top. Catal.* **2023**, *66*, 1527.
- [137] T. Akter, H. Pan, C. J. Barile, *J. Phys. Chem. C* **2022**, *126*, 10045.
- [138] X. She, L. Zhai, Y. Wang, P. Xiong, M. M.-J. Li, T.-S. Wu, M. C. Wong, X. Guo, Z. Xu, H. Li et al., *Nat. Energy* **2024**, *9*, 81.
- [139] T. Möller, M. Filippi, S. Brückner, W. Ju, P. Strasser, *Nat. Commun.* **2023**, *14*, 5680.
- [140] Y.-C. Zhang, X.-L. Zhang, Z.-Z. Wu, Z.-Z. Niu, L.-P. Chi, F.-Y. Gao, P.-P. Yang, Y.-H. Wang, P.-C. Yu, J.-W. Duanmu et al., *PNAS* **2024**, *121*, e2400546121.
- [141] P. Izadi, J. Song, C. Singh, D. Pant, F. Harnisch, *Adv. Energy Sustain. Res.* **2024**, *5*, 2400031.
- [142] J. W. Duanmu, Z.-Z. Wu, F.-Y. Gao, P.-P. Yang, Z.-Z. Niu, Y.-C. Zhang, L.-P. Chi, M.-R. Gao, *Precis. Chem.* **2024**, *2*, 151–160.

Manuscript received: August 28, 2024  
Revised manuscript received: October 22, 2024  
Version of record online: December 12, 2024